Table 2 MnSOD, CuZnSOD and GPx activities, and GSH content in HepG2 cells cultured under the indicated conditions

Control, conventional 10% FBS; GSH-deficiency, +5 mM BSO; selenium-deficiency, 1% FBS; selenium replenishment, added 1 μM sodium selenite to selenium-deficient medium.

Conditions	MnSOD (units/mg of protein)	CuZnSOD (units/mg of protein)	GPx (m-units/mg of protein)	GSH (μg/mg protein)
Control	20.9 ± 0.6	21.5 ± 1.0	11.2 ± 0.2	12.1 ± 1.4
(+)5 mM BSO	19.2 ± 0.4	20.8 ± 1.7	9.8 ± 0.3	0.2 ± 0.0
1% FBS	24.9 ± 0.4	18.9 ± 1.1	1.8 ± 0.3	11.6 ± 1.0
1% FBS + Se	24.4 ± 0.5	16.5 ± 1.5	64.3 ± 1.4	9.6 ± 1.3

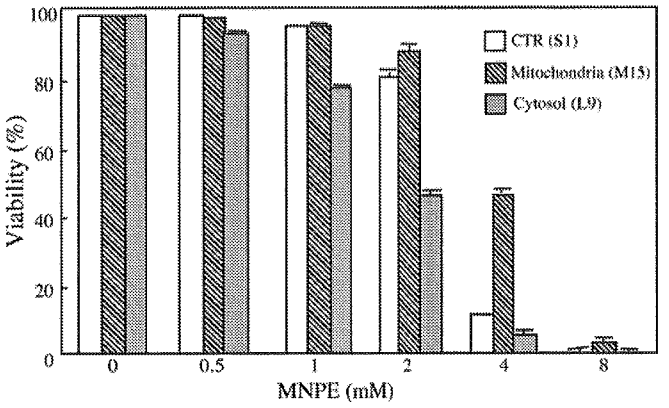

Figure 3 Effects of endoperoxides on cells overexpressing PHGPx

Cells overexpressing PHGPx at cytoplasm (L9 cells, grey bars) or mitochondria (M15 cells, hatched bars) and control cells (S1 cells, open bars) were treated with various concentrations of MNPE for 2 h. After 22 h, viability of the cells was assessed by measuring LDH activity. CTR, control.

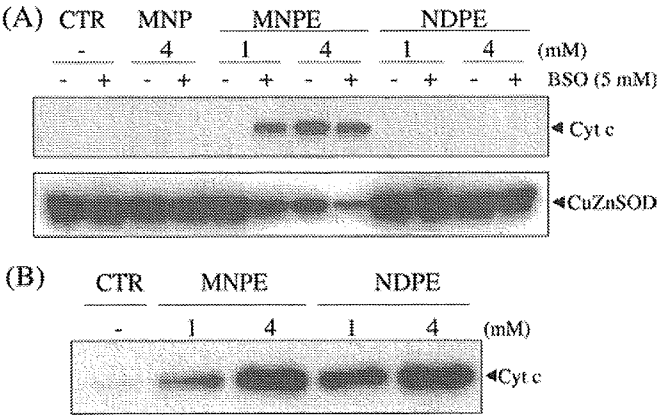

Figure 4 Effect of the endoperoxides on cytochrome *c* release from mitochondria in cells and isolated mitochondria in the cell-free system

(**A**) After treatment with 1 or 4 mM endoperoxides or 4 mM MNP for 2 h, the cytosolic fraction was prepared from HepG2 cells by gentle homogenization in a Dounce homogenizer. Cytochrome *c*, present in the cytosolic fraction, was assayed by immunoblotting using an anti-(cytochrome *c*) (Cyt c) antibody. CuZnSOD was detected by a specific antibody and was used as a marker for cytosolic proteins. (**B**) The mitochondrial fraction was prepared from rat liver by gentle homogenization, followed by centrifugation, and was treated with MNPE or NDPE. After centrifugation, the released cytochrome *c* from mitochondria was analysed by immunoblotting as described above. Typical data from triplicate experiments are shown. CTR, control.

would be limited by the low GSH content within the cells. These data suggest a pivotal role of GSH-dependent detoxification of peroxides in protection against the toxicity of singlet oxygen.

Cells overexpressing PHGPx (phospholipid hydroperoxide GPx) in mitochondria are resistant to singlet oxygen toxicity

Singlet oxygen might increase the formation of peroxides, and PHGPx, among the GPx family members, is generally thought to play a significant role in protection against the ROS cytotoxicity [35]. We examined the cytotoxic effects of MNPE on control cells (S1), which were transfected with vector alone, or cells overexpressing PHGPx either at the cytoplasm (L9) or at the mitochondria (M15) [36,37] (Figure 3). The results showing that M15 cells were the most resistant to the cytotoxic effects of MNPE point to mitochondria as a potential target for singlet oxygen. It is not clear at present, however, why cells that express more PHGPx in the cytoplasm are less resistant to cytotoxicity than control cells.

Effect of endoperoxides on the cytochrome *c* release from mitochondria

Since mitochondria appeared to be a target of singlet oxygen, we examined the levels of both cytochrome *c* released into cytoplasm and the portion remaining in mitochondria in cells after treatment with the endoperoxides. While the treatment of cells with MNPE caused the release of cytochrome *c* into the cytoplasm, no cytochrome *c* release was observed in the cytoplasm of cells treated with either NDPE or MNP (Figure 4A). These data indicate that the observed cytotoxic effect can be attributed to singlet oxygen generated from MNPE located near the mitochondria in cells. The depletion of glutathione by treatment with BSO enhanced the release of cytochrome *c*. This is consistent with the cytoprotective role of glutathione against singlet-oxygen-induced damage. Thus, despite the similar chemical nature of the two endoperoxides as singlet oxygen donors, only MNPE effectively impaired mitochondria and triggered the release of cytochrome *c* in cells.

To examine the potential detrimental effects of endoperoxides on mitochondria, we investigated their direct action on isolated mitochondria from rat liver (Figure 4B). Both MNPE and NDPE triggered the release of cytochrome *c* from isolated mitochondria to almost the same extent. This mitochondrial toxicity of both endoperoxides observed in the cell-free system suggest that the above results obtained in cultured cells are related to the membrane permeability of the compounds, i.e. MNPE penetrated the plasma membrane and reached the mitochondria, but NDPE did not.

Characterization of cellular damage caused by singlet oxygen

To gain insight into the mechanism of cell death, morphological changes in the cells were observed and compared with those during etoposide-induced apoptosis. When the cells were stained with DAPI and examined by fluorescence microscopy, condensed chromatin and fragmented nuclei, which are criteria for apoptosis,

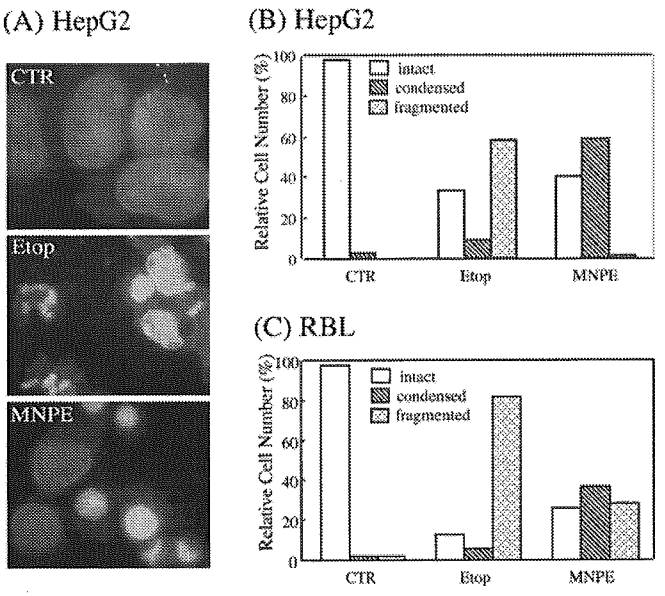

Figure 5 Singlet oxygen induced chromatin condensation, but not nuclear fragmentation

HepG2 cells were incubated with 0.4 mM etoposide (Etop) throughout the period or 2 mM MNPE for 2 h. After 16 h, the cells were stained with DAPI and examined under a fluorescence microscope (**A**). The number of intact, condensed, and fragmented nuclei of HepG2 (**B**) or RBL (**C**) cells were counted in more than 500 cells and the data are presented as a percentage. CTR, control.

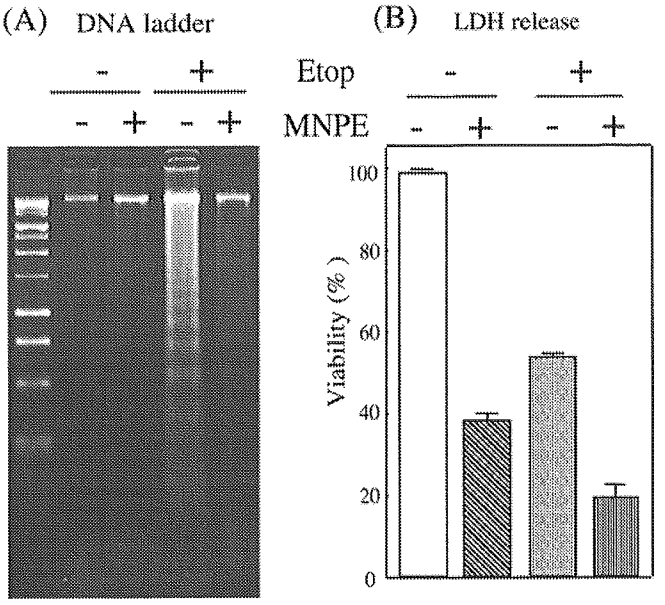

Figure 6 Effects of singlet oxygen on DNA ladder formation

RBL cells were incubated with 2 mM MNPE for an initial 2 h, changed to fresh medium, and incubated an additional 15 h. For etoposide treatment, 0.4 mM etoposide (Etop) was present all the time. MNPE (2 mM) was included from 3 to 5 h after etoposide addition, and the cells were incubated further for an additional 13 h in fresh medium containing etoposide. (**A**) DNA was extracted from cells, separated on a 2 % agarose gel and stained with ethidium bromide. Typical data of triplicate experiments are shown. (**B**) Viability of cells that had been treated under the same conditions as (**A**) was assessed by measuring LDH activity.

were observed in these cells (Figure 5A). The number of cells that contained either condensed chromatin or fragmented nuclei were counted and compared. When HepG2 cells were treated with etoposide, approx. 60 % contained fragmented nuclei. However, treatment with MNPE decreased the number of cells with fragmented nuclei and increased those with condensed nuclei (Figure 5B). Although their population was different, a similar trend was observed in RBL cells by treatment with MNPE (Figure 5C). Since nuclear fragmentation follows chromatin condensation in apoptosis, the morphological process characteristic of apoptosis appeared to cease at this stage during the cell death caused by singlet oxygen.

We characterized further the nature of the cellular damage by assaying DNA fragmentation, another criterion of apoptosis. DNA, prepared from RBL cells that had been treated with etoposide and/or MNPE, was run on an agarose gel (Figure 6A). Although the viability of cells was slightly different between the two groups, DNA ladder formation was much less in MNPE-treated cells than in etoposide-treated cells (Figure 6B). The presence of MNPE for the initial 2 h during etoposide treatment suppressed DNA ladder formation. When a FACS analysis was performed using propidium iodide and annexin V staining, the population of the propidium-iodide-negative and annexin-V-positive cells, corresponding to apoptotic cells, was decreased with a parallel increase in double positive cells, corresponding to necrotic cells, in MNPE-treated cells compared with etoposide-treated cells (results not shown). These data indicate that cells treated with MNPE released cytochrome *c* from the mitochondria, but did not undergo typical apoptotic death.

Singlet oxygen inhibits caspase activity

Since DNA fragmentation and the accompanying apoptotic process triggered by many stimuli is mediated by activation of the caspase cascade after the release of cytochrome *c* into the cytosol, we examined the caspase activity of cytosolic fractions from HepG2 cells that had been treated with MNPE and compared the findings with that from etoposide-treated cells (Figure 7). The activities of both caspase 9 and caspase 3 were gradually elevated, reaching a maximum at 17 h after etoposide treatment. In MNPE-treated cells, however, their activities were much lower than those of etoposide-treated cells through this period.

Proteins, as well as caspase 9 and 3 activities, were then assayed in HepG2 cells that had been treated with MNPE and/or etoposide (Figure 8). While both activities were markedly elevated in etoposide-treated cells, the activities in MNPE-treated cells were again very low (Figure 8A). The co-presence of MNPE from 15 to 17 h after etoposide addition significantly suppressed their activities. An immunoblot analysis of the cytosolic proteins showed that the caspase activity roughly corresponded to the processing of precursors to mature forms (Figure 8B). The low level of cleaved PARP, a nuclear protein and predominant substrate of caspase 3, was also consistent with a low caspase 3 activity in the MNPE-treated cells.

Singlet oxygen suppresses activation of the caspase cascade

To elucidate the mechanism associated with the low caspase activity in MNPE-treated cells, we extracted soluble proteins from etoposide-treated cells and incubated them with MNPE (Figure 9). The effects of treatment with SNAP, an NO donor, and 10 mM DTT were also examined. When the protein fraction that originally contained high caspase activities was treated with MNPE, a marked suppression of the activity was observed (Figure 9A). The inhibition was dose-dependent, with a half-maximal inhibition at approx. 1 mM MNPE under these conditions (Figure 9B). A buffer pH between 6 and 9 during treatment with MNPE did not significantly affect the inhibition, although a lower pH caused a decrease in activity (results not shown). Reduction with DTT

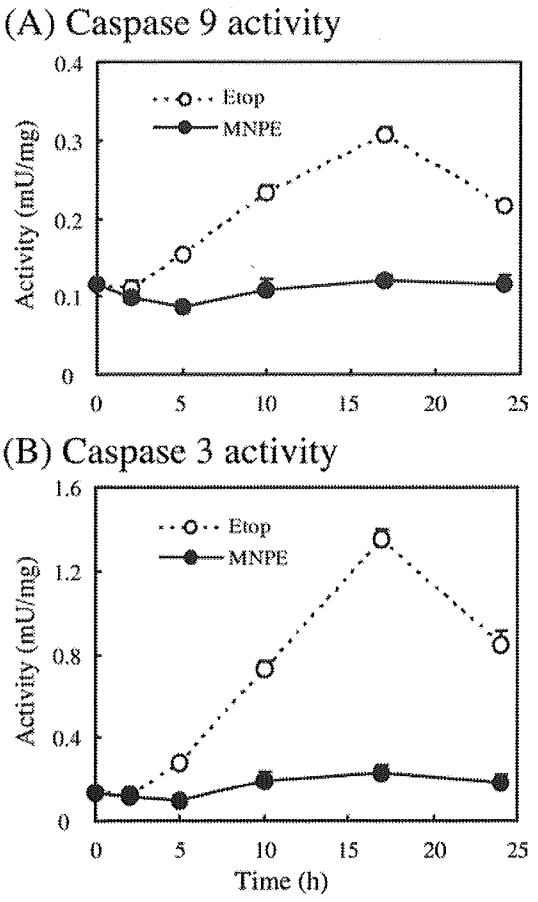

Figure 7 Comparison of activities of caspase 9 and 3 between etoposide- and singlet-oxygen-induced cell death

HepG2 cells were incubated with 2 mM MNPE for an initial 2 h, changed to fresh medium, and incubated for an additional 15 h. For etoposide treatment, 0.5 mM etoposide (Etop) was present at all times. A cellular lysate was prepared at the indicated time points. Activities of caspase 9 (**A**) and 3 (**B**) were assayed using specific substrates.

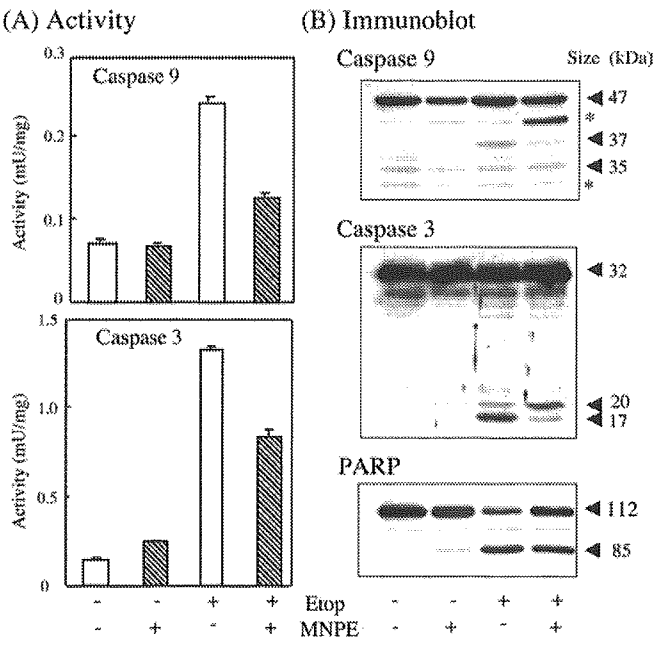

Figure 8 Correlation of activities of caspase 9 and 3 with their active forms and PARP

(**A**) HepG2 cells were incubated with 2 mM MNPE for an initial 2 h, changed to fresh medium, and incubated for an additional 15 h. With etoposide treatment, 0.4 mM etoposide (Etop) was present all the time. MNPE was added to 2 mM at 15 h after etoposide and incubated further for 2 h. (**B**) Approx. 10 μg of protein was separated by SDS/PAGE and blotted on to a Hybond-P membrane. Immunoblot analyses were performed using anti-(caspase 9), anti-(caspase 3) or anti-PARP antibodies. Typical data from triplicate experiments are shown. Sizes of proteins are shown in kDa. *, non-specific band.

only slightly recovered the activity (Figure 9C). We then examined the effects of MNPE on caspase activities in a cell-free system that had been reconstituted from the cytosolic fraction, cytochrome *c*, dATP and magnesium. Full activity was obtained when all these components were included in the cytosolic fraction. The presence of MNPE as well as SNAP also suppressed the activation of caspases 9 and 3 in the cell-free reconstitution system (Figure 9D). Thus treatment with singlet oxygen appeared to suppress activation of the caspase cascade by activators of apoptosome formation.

We also examined the effects of pre-treating the cells with MNPE on the activation of the caspase cascade in a cell-free system (Figure 10). After 2 h of incubation of HepG2 cells with 2 mM MNPE, the cytosolic fraction was obtained and was stimulated with activators. The activities of caspase 9 and 3 were much lower in MNPE-treated cells than in untreated cells (Figure 10A). The levels of active forms of caspase 9 and 3 present were consistent with their low activities (Figure 10B). Thus singlet oxygen suppressed the activation of the caspase cascade before the processing of caspase 9.

DISCUSSION

We synthesized and used two naphthalene endoperoxides with different polarities, but a similar half-life as singlet oxygen donors, and found that only the less polar donor MNPE damaged the cells (Figure 1). This suggests that the production of singlet oxygen in close proximity to the target molecule in cells is required to exert a detrimental effect. Klotz et al. [19] reported a similar observation for HL-60 cells using different endoperoxides.

The suppression of GPx activity in cells either by decreasing FBS supplementation to 1 %, which decreased GPx proteins, or by the inhibition of GSH biosynthesis by BSO treatment (Table 1) enhanced the sensitivity of the cells to singlet oxygen toxicity (Figure 2). Although GPx activity, which was measured in the presence of a large excess of GSH, was similar to the control, the capacity of the GSH-dependent detoxification of peroxides would be limited in GSH-deficient cells. The reactivity of singlet oxygen to the conjugated double bond is very high ($\sim 10^6$ $M^{-1} \cdot s^{-1}$) and, hence, causes lipid peroxidation [1]. Although singlet oxygen is not a radical and cannot be directly detoxified by antioxidative enzymes, ROS that are generated by reactions with singlet oxygen in cells may exert harmful effects. Thus the resulting ROS, but not singlet oxygen itself, could be a substrate in the GSH-dependent detoxification reaction.

When intact cells were treated with these endoperoxides, only the less polar MNPE was effective. The half-life of singlet oxygen in water is several microseconds, and thus the distance it can penetrate is less than 50 nm. In addition, the plasma membrane contains many singlet-oxygen-scavenging compounds, e.g. vitamin E, which would decrease the amount of singlet oxygen within the lipid bilayer. Thus singlet oxygen produced near a target molecule would be effective. Mitochondria were shown to be one of the primary targets of singlet oxygen within cells (Figures 3 and 4). However, both compounds were equally effective on isolated

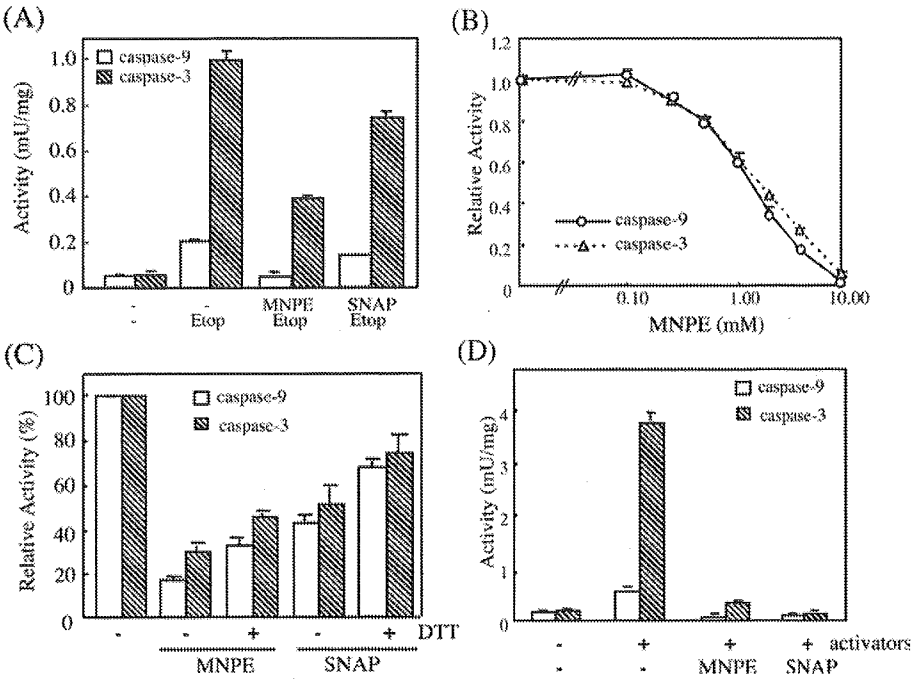

Figure 9 Effects of singlet oxygen and NO on caspase activities from cells pre-treated with etoposide, and the effects of reduction with DTT

(**A**)–(**C**) Apoptosis was induced by 0.4 mM etoposide in HepG2 cells. Activities of caspase 9 and 3 were measured in cytosolic fractions of the cells that had been treated as follows. (**A**) Cytosolic fractions were incubated further with 2 mM MNPE or 2 mM SNAP for 2 h at 37 °C. (**B**) Cytosolic fractions were treated with various concentrations of MNPE for 2 h at 37 °C. (**C**) After treatment of the cytosolic fraction with either 2 mM MNPE or 2 mM SNAP as in (**A**), cytosolic fractions were incubated further with 10 mM DTT for 1 h at 37 °C. (**D**) The cytosolic fraction was prepared from untreated HepG2 cells. The caspase cascade was activated by adding activators, cytochrome *c*, dATP and $MgCl_2$. Effects of 2 mM MNPE or 2 mM SNAP on caspase activities were examined in samples by co-incubation with these activators.

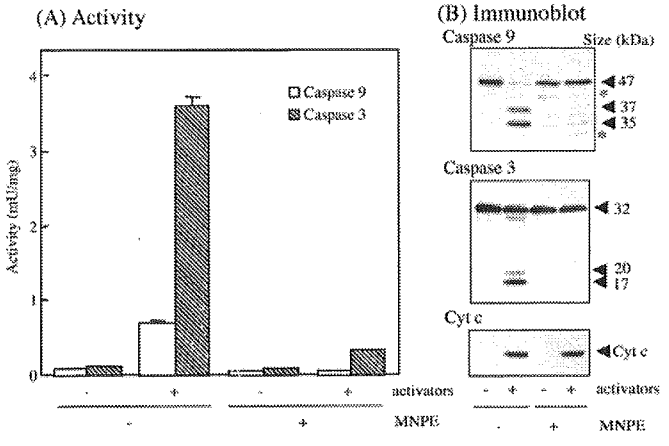

Figure 10 Effects of pre-treatment of cells with MNPE on caspase activation in the cell-free system

HepG2 cells were pre-treated without (−) or with (+) 2 mM MNPE for 2 h, and cytosolic fractions were prepared immediately. Caspases in the fractions were activated by adding activators, cytochrome *c*, dATP and $MgCl_2$. (**A**) Activities of caspase 9 and 3 were measured in triplicate. (**B**) Approx. 10 μg of protein was separated by SDS/PAGE and blotted on to the Hybond-P membrane. Immunoblot analyses were performed using the anti-(caspase 9), anti-(caspase 3) or anti-(cytochrome *c*) antibody. Sizes of proteins are shown in kDa. *, non-specific band. Typical data of triplicate experiments are shown.

mitochondria from rat liver. This indicates that the generation of ROS near the mitochondria would be required for singlet oxygen to exert cytotoxicity. Damage of the target molecule by singlet oxygen in mitochondria is considered to be directly or indirectly involved in the release of cytochrome *c*. Taking the high reactivity of singlet oxygen to the conjugated double bond into consideration, the most likely target in mitochondria are molecules containing polyunsaturated fatty acids. When we evaluated the effects of singlet oxygen, cells that express high levels of PHGPx in mitochondria exhibited the highest resistance to MNPE (Figure 3). The protection of cells by PHGPx from damage during photodynamic therapy has been documented [38]. The peroxidation of cardiolipin, a lipid that is predominantly present in the mitochondrial inner membrane and which is rich in unsaturated fatty acid, is a possible mechanism of cytochrome *c* release during oxidative stress in mitochondria [39,40]. Hence, PHGPx is likely to protect mitochondria by preventing this particular lipid from peroxidation triggered by singlet oxygen. The protective role of vitamin E against MNPE may be explained by high efficiency in incorporation into cells compared with β-carotene (Table 1). It is also possible that vitamin E interacts with MNPE and affects the generation of singlet oxygen.

Regarding cellular damage by singlet oxygen, several cytotoxic mechanisms have been proposed. Mitogen-activated protein kinases, p38, JNK and ERK, are activated during apoptosis induced by singlet oxygen and UV [18,19,21,41,42]. The involvement of transcription factors, such as AP-2 (activator protein 2), is also known [43]. In singlet-oxygen-induced cell damage, apoptotic machinery would be initiated by the cytochrome *c* released into the cytosol. The damaged cells showed chromatin condensation, a morphological profile of apoptotic cell death. However, we observed only very low levels of nuclear fragmentation (Figure 5). It appears that cellular damage ceased at the stage of chromatin condensation. On the other hand, DNA ladder formation, another criterion of apoptosis, was also suppressed in MNPE-treated cells (Figure 6). Thus these characteristics of cell death triggered by singlet oxygen were different from typical apoptosis.

To investigate the molecular mechanism of this atypical cell death, we examined caspase activities. When cells were treated with MNPE or etoposide and showed a similar viability as judged by LDH activity, the activities of caspase 9 and 3 were much lower in MNPE-treated cells than in etoposide-treated cells (Figures 7 and 8). The suppression of caspase activities by singlet oxygen appeared to occur by at least two mechanisms in the cell death pathway.

One is the direct action of singlet oxygen on the active forms of caspases. MNPE inhibited the activities of both caspase 9 and 3 directly in cells treated with etoposide or in the cytosolic fraction that contained active forms of caspases, as judged by the presence of processed forms (Figures 8 and 9). At high doses, NO is a well-known cytotoxic mediator and causes cell death. NO is known to cause caspase inhibition by modifying the reactive thiol residue in the catalytic centre [44]. Singlet oxygen, as well as NO, preferentially reacts with deprotonated thiol and results in modification of the reactive residue. Free cysteine reacts with singlet oxygen to give the disulphide and also cysteic acid [14]. Caspases would be a preferable target, because they possess a reactive cysteine residue that is involved in proteolytic reactions. While the inactivation of caspase 3 with H_2O_2 is reversible [45], singlet-oxygen-induced inactivation was only partially reversed by reduction with DTT (Figure 9C). It would be intriguing to know what types of modification actually occur in the case of caspases. However, the reaction of sterically constrained thiol groups in proteins with singlet oxygen has not been investigated extensively [14]. A chemical analysis of the products will be needed to understand the reaction of thiol groups with singlet oxygen.

The other mechanism of caspase suppression would be related to apoptosome formation. The cytochrome *c* released from mitochondria binds Apaf 1 (apoptotic protease-activating factor 1) and forms an apoptosome together with procaspase 9, dATP and other factors [46]. This process appears to be redox-sensitive, because NO modulates the process [47]. We examined the effects of singlet oxygen on caspase activation in a cell-free reconstitution system and observed the suppression of caspase activation by these activators (Figure 9D). Although it would be intriguing to determine the effect of MNPE pre-treatment on the activation of caspases, the caspase cascade was inactivated irreversibly during incubation at 37 °C, even in the absence of MNPE (results not shown). This is because the machinery involved in apoptosome formation is unstable in a cell-free system at 37 °C. Since the release of singlet oxygen from MNPE is highly temperature sensitive and only a very small amount of singlet oxygen was released from MNPE at 4 °C, we were unable to examine the effect of singlet oxygen on apoptosome formation in the MNPE-treated cytosolic fraction. Therefore we examined the effects of singlet oxygen on the activation of the caspase cascade using the cytosolic fraction from the cells pre-treated with MNPE (Figure 10). The activities of caspase 9 and 3, as well as their active forms, implied that singlet oxygen suppressed the activation of the caspase cascade. It has been shown that some of the products formed on the reaction of singlet oxygen with amino acids and peptides can have potent inhibitory effects on caspase activity [48]. It is therefore possible that the observed inhibition of caspase activity may not be directly mediated by singlet oxygen, but arise from some of its downstream products [49].

Another question is what is the fate of cells undergoing abortive apoptosis? *In vivo*, cells can be efficiently phagocytosed without the translocation of phosphatidylserine to the outer leaflet of the plasma membrane [50]. In addition, the involvement of other proteases in the process has been documented [51]. It has actually been reported that caspase activation is not required for apoptosis of a certain type of cells [52]. Our data also show that singlet oxygen caused cell death that was not typical apoptosis owing to the suppression of caspase activity.

In conclusion, single oxygen intracellularly generated from endoperoxides caused cell death. One of the primary target organelles within cells is the mitochondrion. Although singlet oxygen reacts with several cellular components, such as polyunsaturated fatty acids, that are involved in the retention of cytochrome *c* in the inner membrane are the likely targets. Caspase activities did not correspond to the levels of released cytochrome *c* in the cytoplasm. This is mainly due to the impairment of caspases by singlet oxygen. Consequently, the cells did not follow a typical apoptotic pathway, but showed an atypical, necrosis-like cell death.

We thank Ms Masako Seki for maintenance of laboratory equipment and secretarial services. This work was supported, in part, by Grant-in-Aid for Scientific Research (C) (No. 16590238) and 21st Century COE Program from the Japan Society for the Promotion of Science (JSPS) and by the Ichiro Kanehara Foundation.

REFERENCES

1 Halliwell, B. and Gutteridge, J. M. C. (1999) Free Radical Biology and Medicine, 3rd edn. Clarendon Press, Oxford
2 Green, D. and Reed, J. C. (1998) Mitochondria and apoptosis. Science **281**, 1309–1312
3 Hengartner, M. O. (2000) The biochemistry of apoptosis. Nature (London) **407**, 770–776
4 Cain, K., Bratton, S. B., Langlais, C., Walker, G., Brown, D. G., Sun, X. M. and Cohen, G. M. (2000) Apaf-1 oligomerizes into biologically active approximately 700-kDa and inactive approximately 1.4-MDa apoptosome complexes. J. Biol. Chem **275**, 6067–6070
5 Khan, A. U. and Kasha, M. (1994) Singlet molecular oxygen in the Haber–Weiss reaction. Proc. Natl. Acad. Sci. U.S.A. **91**, 12365–12367
6 Khan, A. U., Kovacic, D., Kolbanovskiy, A., Desai, M., Frenkel, K. and Geacintov, N. E. (2000) The decomposition of peroxynitrite to nitroxyl anion (NO^-) and singlet oxygen in aqueous solution. Proc. Natl. Acad. Sci. U.S.A. **97**, 2984–2989
7 Berneburg, M., Grether-Beck, S., Kurten, V., Ruzicka, T., Briviba, K., Sies, H. and Krutmann, J. (1999) Singlet oxygen mediates the UVA-induced generation of the photoaging-associated mitochondrial common deletion. J. Biol. Chem. **274**, 15345–15349
8 Ahmad, N. and Mukhtar, H. (2000) Mechanism of photodynamic therapy-induced cell death. Methods Enzymol. **319**, 342–358
9 Tatsuzawa, H., Maruyama, T., Misawa, N., Fujimori, K., Hori, K., Sano, Y., Kambayashi, Y. and Nakano, M. (1998) Inactivation of bacterial respiratory chain enzymes by singlet oxygen. FEBS Lett. **439**, 329–333
10 Tatsuzawa, H., Maruyama, T., Hori, K., Sano, Y. and Nakano, M. (1999) Singlet oxygen ($^1\Delta_g O_2$) as the principal oxidant in myeloperoxidase-mediated bacterial killing in neutrophil phagosome. Biochem. Biophys. Res. Commun. **262**, 647–650
11 Tatsuzawa, H., Maruyama, T., Misawa, N., Fujimori, K. and Nakano, M. (2000) Quenching of singlet oxygen by carotenoids produced in *Escherichia coli* – attenuation of singlet oxygen-mediated bacterial killing by carotenoids. FEBS Lett. **484**, 280–284
12 Pellieux, C., Dewilde, A., Pierlot, C. and Aubry, J. M. (2000) Bactericidal and virucidal activities of singlet oxygen generated by thermolysis of naphthalene endoperoxides. Methods Enzymol. **319**, 197–207
13 Petrat, F., Pindiur, S., Kirsch, M. and de Groot, H. (2003) NAD(P)H, a primary target of $^1O_2$ in mitochondria of intact cells. J. Biol. Chem. **278**, 3298–3307
14 Davies, M. J. (2003) Singlet oxygen-mediated damage to proteins and its consequences. Biochem. Biophys. Res. Commun. **305**, 761–770
15 Morita, A., Werfel, T., Stege, H., Ahrens, C., Karmann, K., Grewe, M., Grether-Beck, S., Ruzicka, T., Kapp, A., Klotz, L. O. et al. (1997) Evidence that singlet oxygen-induced human T helper cell apoptosis is the basic mechanism of ultraviolet-A radiation phototherapy. J. Exp. Med. **186**, 1763–1768
16 Godar, D. E. (1999) UVA1 radiation triggers two different final apoptotic pathways. J. Invest. Dermatol. **112**, 3–12
17 Kochevar, I. E., Lynch, M. C., Zhuang, S. and Lambert, C. R. (2000) Singlet oxygen, but not oxidizing radicals, induces apoptosis in HL-60 cells. Photochem. Photobiol. **72**, 548–553
18 Klotz, L. O., Briviba, K. and Sies, H. (1997) Singlet oxygen mediates the activation of JNK by UVA radiation in human skin fibroblasts. FEBS Lett. **408**, 289–291
19 Klotz, L. O., Pellieux, C., Briviba, K., Pierlot, C., Aubry, J. M. and Sies, H. (1999) Mitogen-activated protein kinase (p38-, JNK-, ERK-) activation pattern induced by extracellular and intracellular singlet oxygen and UVA. Eur. J. Biochem. **260**, 917–922

20 Klotz, L. O. (2002) Oxidant-induced signaling: effects of peroxynitrite and singlet oxygen. Biol. Chem. **383**, 443–456
21 Zhuang, S., Demirs, J. T. and Kochevar, I. E. (2000) p38 mitogen-activated protein kinase mediates bid cleavage, mitochondrial dysfunction, and caspase-3 activation during apoptosis induced by singlet oxygen but not by hydrogen peroxide. J. Biol. Chem. **275**, 25939–25948
22 Aubry, J. M., Cazin, B. and Duprat, F. (1989) Chemical sources of singlet oxygen. 3. Peroxidation of water-soluble singlet oxygen carriers with the hydrogen peroxide–molybdate system. J. Org. Chem. **54**, 726–728
23 Liu, W., Ogata, T., Sato, K., Ohba, Y., Sakurai, K. and Igarashi, T. (2001) Syntheses of water-soluble endoperoxides as a singlet oxygen source. ITE Lett. Batt. New Technol. Med. **2**, 98–101
24 Saito, I., Matsuura, T. and Inoue, K. (1983) Formation of superoxide ion via one-electron transfer from electron donors to singlet oxygen. J. Am. Chem. Soc. **105**, 3200–3206
25 Nakano, M., Kambayashi, Y., Tatsuzawa, H., Komiyama, T. and Fujimori, K. (1998) Useful $^1O_2$ ($^1\Delta_g$) generator, 3-(4′-methyl-1′-naphthyl)-propionic acid, 1′,4′-endoperoxide (NEPO), for dioxygenation of squalene (a skin surface lipid) in an organic solvent and bacterial killing in aqueous medium. FEBS Lett. **432**, 9–12
26 Solichova, D., Korecka, L., Svobodova, I., Musil, F., Blaha, V., Zdansky, P. and Zadak, Z. (2003) Development and validation of HPLC method for the determination of α-tocopherol in human erythrocytes for clinical applications. Anal. Bioanal. Chem. **376**, 444–447
27 Offord, E. A., Gautier, J. C., Avanti, O., Scaletta, C., Runge, F., Kramer, K. and Applegate, L. A. (2002) Photoprotective potential of lycopene, β-carotene, vitamin E, vitamin C and carnosic acid in UVA-irradiated human skin fibroblasts. Free Radical Biol. Med. **32**, 1293–1303
28 Kayanoki, Y., Fujii, J., Islam, K. N., Suzuki, K., Kawata, S., Matsuzawa, Y. and Taniguchi, N. (1996) The protective role of glutathione peroxidase in apoptosis induced by reactive oxygen species. J. Biochem. (Tokyo) **119**, 817–822
29 Anderson, M. E. (1985) Determination of glutathione and glutathione disulfide in biological samples. Methods Enzymol. **113**, 548–555
30 Otsu, K., Ikeda, Y. and Fujii, J. (2004) Accumulation of manganese superoxide dismutase under metal-depleted conditions: proposed role for zinc ions in cellular redox balance. Biochem. J. **377**, 241–248
31 Stennicke, H. R. and Salvesen, G. S. (1997) Biochemical characteristics of caspases-3, -6, -7, and -8. J. Biol. Chem. **272**, 25719–25723
32 Matsuki, S., Iuchi, Y., Ikeda, Y., Sasagawa, I., Tomita, Y. and Fujii, J. (2003) Suppression of cytochrome *c* release and apoptosis in testes with heat stress by minocycline. Biochem. Biophys. Res. Commun. **312**, 843–849
33 Ishizawa, M., Kobayashi, Y., Miyamura, T. and Matsuura, S. (1991) Simple procedure of DNA isolation from human serum. Nucleic Acids Res. **19**, 5792
34 Cain, K., Brown, D. G., Langlais, C. and Cohen, G. M. (1999) Caspase activation involves the formation of the aposome, a large (approximately 700 kDa) caspase-activating complex. J. Biol. Chem. **274**, 22686–22692
35 Imai, H. and Nakagawa, Y. (2003) Biological significance of phospholipid hydroperoxide glutathione peroxidase (PHGPx, GPx4) in mammalian cells. Free Radical Biol. Med. **34**, 145–169
36 Arai, M., Imai, H., Koumura, T., Yoshida, M., Emoto, K., Umeda, M., Chiba, N. and Nakagawa, Y. (1999) Mitochondrial phospholipid hydroperoxide glutathione peroxidase plays a major role in preventing oxidative injury to cells. J. Biol. Chem. **274**, 4924–4933
37 Nomura, K., Imai, H., Koumura, T., Arai, M. and Nakagawa, Y. (1999) Mitochondrial phospholipid hydroperoxide glutathione peroxidase suppresses apoptosis mediated by a mitochondrial death pathway. J. Biol. Chem. **274**, 29294–29302
38 Wang, H. P., Qian, S. Y., Schafer, F. Q., Domann, F. E., Oberley, L. W. and Buettner, G. R. (2001) Phospholipid hydroperoxide glutathione peroxidase protects against singlet oxygen-induced cell damage of photodynamic therapy. Free Radical Biol. Med. **30**, 825–835
39 Nomura, K., Imai, H., Koumura, T., Kobayashi, T. and Nakagawa, Y. (2000) Mitochondrial phospholipid hydroperoxide glutathione peroxidase inhibits the release of cytochrome *c* from mitochondria by suppressing the peroxidation of cardiolipin in hypoglycaemia-induced apoptosis. Biochem. J. **351**, 183–193
40 Petrosillo, G., Ruggiero, F. M. and Paradies, G. (2003) Role of reactive oxygen species and cardiolipin in the release of cytochrome *c* from mitochondria. FASEB J. **17**, 2202–2208
41 Chan, W. H., Yu, J. S. and Yang, S. D. (2000) Apoptotic signalling cascade in photosensitized human epidermal carcinoma A431 cells: involvement of singlet oxygen, c-Jun N-terminal kinase, caspase-3 and p21-activated kinase 2. Biochem. J. **351**, 221–232
42 Zhuang, S., Lynch, M. C. and Kochevar, I. E. (1999) Caspase-8 mediates caspase-3 activation and cytochrome *c* release during singlet oxygen-induced apoptosis of HL-60 cells. Exp. Cell Res. **250**, 203–212
43 Grether-Beck, S., Olaizola-Horn, S., Schmitt, H., Grewe, M., Jahnke, A., Johnson, J. P., Briviba, K., Sies, H. and Krutmann, J. (1996) Activation of transcription factor AP-2 mediates UVA radiation- and singlet oxygen-induced expression of the human intercellular adhesion molecule 1 gene. Proc. Natl. Acad. Sci. U.S.A. **93**, 14586–14591
44 Li, J., Bombeck, C. A., Yang, S., Kim, Y. M. and Billiar, T. R. (1999) Nitric oxide suppresses apoptosis via interrupting caspase activation and mitochondrial dysfunction in cultured hepatocytes. J. Biol. Chem. **274**, 17325–17333
45 Borutaite, V. and Brown, G. C. (2001) Caspases are reversibly inactivated by hydrogen peroxide. FEBS Lett. **500**, 114–118
46 Zou, H., Li, Y., Liu, X. and Wang, X. (1999) An APAF-1 · cytochrome *c* multimeric complex is a functional apoptosome that activates procaspase-9. J. Biol. Chem. **274**, 11549–11556
47 Zech, B., Köhl, R., von Knethen, A. and Brüne, B. (2003) Nitric oxide donors inhibit formation of the Apaf-1/caspase-9 apoptosome and activation of caspases. Biochem. J. **371**, 1055–1064
48 Hampton, M. B., Morgan, P. E. and Davies, M. J. (2002) Inactivation of cellular caspases by peptide-derived tryptophan and tyrosine peroxides. FEBS Lett. **527**, 289–292
49 Davies, M. J. (2004) Reactive species formed on proteins exposed to singlet oxygen. Photochem. Photobiol. Sci. **3**, 17–25
50 Leist, M. and Jaattela, M. (2001) Four deaths and a funeral: from caspases to alternative mechanisms. Nat. Rev. Mol. Cell Biol. **2**, 589–598
51 Foghsgaard, L., Wissing, D., Mauch, D., Lademann, U., Bastholm, L., Boes, M., Elling, F., Leist, M. and Jaattela, M. (2001) Cathepsin B acts as a dominant execution protease in tumor cell apoptosis induced by tumor necrosis factor. J. Cell Biol. **153**, 999–1010
52 McCarthy, N. J., Whyte, M. K., Gilbert, C. S. and Evan, G. I. (1997) Inhibition of Ced-3/ICE-related proteases does not prevent cell death induced by oncogenes, DNA damage, or the Bcl-2 homologue Bak. J. Cell Biol. **136**, 215–227

Received 13 December 2004/9 March 2005; accepted 16 March 2005
Published as BJ Immediate Publication 30 March 2005, DOI 10.1042/BJ20042067

GFRR 113034—29/4/2005—SRIVIDYAR—146392

Free Radical Research, Month 2005; 00(0): 1–9

Accelerated impairment of spermatogenic cells in sod1-knockout mice under heat stress

TATSUYA ISHII[1,2], SHINGO MATSUKI[1,2], YOSHIHITO IUCHI[1], FUTOSHI OKADA[1], SHINJIRO TOYOSAKI[1], YOSHIHIKO TOMITA[2], YOSHITAKA IKEDA[3], & JUNICHI FUJII[1]

[1]*Department of Biomolecular Function, Graduate School of Medical Science, Yamagata University, Yamagata, Japan,* [2]*Department of Urology, Yamagata University School of Medicine, 2-2-2 Iidanishi, Yamagata 990-9585, Japan, and* [3]*Division of Molecular Cell Biology, Department of Biomolecular Sciences, Saga University Faculty of Medicine, 5-1-1 Nabeshima, Saga 849-8501, Japan*

Accepted by Dr J. Yodi

(Received 17 November 2004; in revised form 4 April 2005)

Abstract

For normal spermatogenesis, the temperature of the scrotum is lower than that of the body. The mechanism by which mammalian testes undergoes cell death as the result of exposure to heat continues to be a matter of debate. Since generation of reactive oxygen species (ROS) during heat stress and involvement in spermatogenic cell damage are postulated, we induced experimental cryptorchidism in the testes of SOD1-knockout mice and examined effects of the gene deficiency. The cleavage of DNA in testicular cells, as judged by TUNEL staining, were elevated in SOD1-knockout mice at an earlier stage than in the wild-type mice. To confirm responsiveness of SOD1 for this high susceptibility to heat stress, spermatogenic cells were isolated from SOD1-knockout and wild-type mice and cultured at 32.5 and 37°C. The cells isolated from SOD1-knockout were more vulnerable at both temperatures than those from wild-type mice. The exposure of cultured rat spermatogenic cells to ROS induced the release of cytochrome c from mitochondria, while Sertoli cells were more resistant under the same conditions. Tiron, a superoxide scavenger, suppressed the heat-induced release of cytochrome c from mitochondria. Collectively, these data suggest that ROS are generated during heat stress and cause spermatogenic cell death. Alternatively, since even a short exposure triggers harmful damage to spermatogenic cells, generated ROS may function as a type of signal for cell death rather than directly causing oxidative damage to cells.

Keywords: *Reactive oxygen species, heat stress, cryptorchidism, super oxide, superoxide dismutase*

Abbreviations: *Cyt c, cytochrome c; DTT, dithiothreitol; FBS, fetal bovine serum; HE, hematoxylin and eosin; PBS, phosphate-buffered saline; PhGPx, phospholipid hydroperoxide glutathione peroxidase; ROS, reactive oxygen species; SDS-PAGE, sodium dodecyl sulfate-polyacrylamide gel electrophoresis; SOD, superoxide dismutase; SOD1-KO, SOD1 knockout; TBST, tris-buffered saline containing 0.1% Tween-20; TUNEL, terminal deoxynucleotidyl transferase-mediated deoxyuridine triphosphate nick end labeling*

Introduction

A temperature lower than that of the body cavity is essential for normal spermatogenesis in the testes. Cryptorchidism is associated with male infertility due to an impairment of the spermatogenic process, leading to infertility. This pathogenesis is mainly attributed to high temperatures, since the *in situ* cooling of abdominal testes in the pig results in normal spermatogenesis [1]. Local heating of the lower abdomen to a temperature of 43°C for 15 min induces apoptosis in germ cells and renders the animal

Correspondence: J. Fujii, Department of Biomolecular Function, Graduate School of Medical Science, Yamagata University, 2-2-2 Iidanishi, Yamagata 990-9585, Japan. Fax: 81 23 628 5230. E-mail: jfujii@med.id.yamagata-u.ac.jp

ISSN 1071-5762 print/ISSN 1029-2470 online © 2005 Taylor & Francis Ltd
DOI: 10.1080/10715760500130517

transiently less fertile [2,3]. The surgical induction of cryptorchidism also causes a disruption in spermatogenesis [4–6]. Pachytene spermatocytes and early spermatids are primarily damaged in experimentally induced cryptorchid testes [7]. The damage is characterized by apoptosis within 2–4 days [7,8], eventually resulting in a germ cell deficiency [9].

However, the molecular basis of heat-induced spermatogenic cell damage is not fully understood, but the involvement of the Fas-ligand/Fas system and an apoptosis-related gene p53 is suspected [10,11]. Some pro- and anti-apoptotic proteins appear to be responsible for intracellular signal transduction in heat stress [12–14]. In addition to these protein factors, reactive oxygen species (ROS) also likely function as mediators of heat-induced germ cell damage. In fact, the generation of ROS [15] and elevations in the levels of lipid peroxidation products [16] have been reported. Thus, heat treatment may trigger oxidative stress which, in turn, has a harmful influence on testes.

A number of proteins play a protective role against ROS that are produced under conditions of oxidative stress. Among them, superoxide dismutase (SOD) is generally thought to play a central role because it scavenges superoxide anions, the initially generated ROS from molecular oxygen in cells [17]. Thus, that SOD plays a role in the male reproductive system is a distinct possibility [18,19]. Although CuZnSOD and MnSOD, encoded by the SOD1 and SOD2 genes, respectively, represent a major intracellular superoxide-scavenging system, the contribution of these proteins varies depending on the types of cells [20]. Contrary to the fact that a mutation in SOD1 is a cause of familial amyotrophic lateral sclerosis (FALS), SOD1-knockout mice grow normally and live healthily under conventional breeding conditions [21]. While female SOD1-KO mice are infertile, and no abnormality in the reproductive system has been reported for male SOD1-KO mice [22,23]. Intervention, however, frequently deteriorates the pathological conditions of SOD1-KO mice more severely than is the case for wild-type mice [24,25].

SOD2-KO mice, on the other hand, show dilated cardiomyopathy and die during the neonatal stage [26]. The overexpression or induction of SOD2 causes cells to become more resistant to various stimuli, such as inflammatory cytokines and toxins [20]. However, transgenic male mice that express higher levels of SOD2 exhibit a decreased fertility, for reasons that are not entirely clear [27].

We recently reported that heat stress at 42°C for 15 min triggers the release of cytochrome c from mitochondria, followed by apoptosis in spermatogenic cells and that this process can be inhibited by minocycline [28]. Here we present data that supports the involvement of ROS in heat-stress induced germ cell damage using SOD1-deficient mice.

Materials and methods

Animals

Male Wistar rats were purchased from Japan SLC (Shizuoka, Japan). Three pairs of hetero B6 SOD1-KO mice, established by Matzuk *et al.* [23], were purchased through Jackson Laboratories (Bar Harbor, ME) and bred in our institute. The animal room climate was kept under specific pathogen free conditions at a constant temperature of 21–23°C with a 12 h alternating light-dark cycle. Animal experiments were performed in accordance with the Declaration of Helsinki under the protocol approved by the Animal Research Committee of this institution.

Preparation of testicular cells

Spermatogenic cells and Sertoli cells were isolated and cultivated by a previously described method [29]. All procedures were performed under sterile conditions. Premature male Wistar rats (40 days of age) or SOD1-KO mice were killed under diethylether anesthesia. The testes were removed and decapsulated mechanically. Seminiferous tubules were gently expressed and incubated in PBS containing 0.25% type I collagenase (Wako) for 15 min at 32.5°C with occasional shaking. The seminiferous tubules were then washed and again incubated in PBS containing 0.25% trypsin (Difco, Detroit, MI) for 15 min at 32.5°C with gentle shaking. The trypsin treatment was terminated by adding fetal bovine serum (FBS; Lifeteck Oriental, Tokyo, Japan) to a level of 10% (v/v). The resulting cell suspension was filtered through a metal mesh to remove cell aggregates and tissue debris. Cells were then collected by centrifugation and suspended in F12—L-15 medium, a 1:1 mixture of Ham's F12 and Lebovitz's L15 (ICN Biochemicals, Aurora) supplemented with 1 mg/ml sodium bicarbonate, 100 U/ml penicillin G, 100 μg/ml streptomycin sulfate, 15 mM Hepes (pH 7.3), and 10% FBS. The concentration of testicular cells in the medium was adjusted to 5×10^6/ml. The cells were incubated at 32.5°C, the optimal temperature for testicular spermatogenic cells, in a humidified atmosphere of 5% CO_2 in air. Cells that were attached to the plastic culture plates after 1 day were defined as Sertoli cells, and non-adhering cells were defined as the spermatogenic cell-rich fraction. For short heat-stressed conditions, cells were cultured at 42°C for 1 h followed by incubation at 32.5°C.

Preparation of cytosolic fraction from cultivated cells

This method is essentially the same as described previously [28]. Cells were incubated in media containing hypoxanthine and xanthine oxidase or exposed to heat at 42°C for 1 h and further

incubated at 32.5°C for 30 min in a CO_2 incubator. Cytosolic fractions were prepared as follows. Cells, 5×10^6, were washed in PBS and suspended in 250 μl of buffer (250 mM sucrose, 50 mM Pipes-KOH, pH 7.4, 50 mM KCl, 5 mM EGTA, 2 mM $MgCl_2$, 1 mM DTT, 1 mM phenylmethylsulfonyl fluoride). After standing for 30 min on ice, the cells were lysed with 10 strokes using pestle B in a Dounce homogenizer. After centrifugation at 14,000*g* for 15 min, the supernatant was regarded as the cytosolic fraction.

SDS-PAGE and immunoblot analysis

SDS-PAGE and immunoblot analyses of testicular proteins were performed as described previously [29]. Protein samples were subjected to 15% SDS-PAGE and then transferred to a Hybond-P membrane (Amersham Pharmacia) under semi-dry conditions by means of a Transfer-blot SD semi-dry transfer cell (Bio-Rad). The membrane was then blocked by incubation with 5% skimmed milk in TBS (150 mM NaCl and 20 mM Tris/HCl, pH 7.6) for 2 h at room temperature. The membranes were then incubated with a monoclonal anti-mouse cytochrome c Ig (Cyt c, 1:1,000 dilution) (Pharmingen, San Diego, USA), polyclonal antibodies to MnSOD [30], Prx1 [31], or β-actin overnight at 4°C. A polyclonal antibody to recombinant human CuZnSOD was raised in rabbit and also used. After washing with tris-buffered saline containing 0.1% Tween-20 (TBST), the membrane was incubated with 1:1,000 diluted horseradish peroxidase-conjugated goat anti-mouse IgG (Santa Cruz Biotechnology, Santa Cruz, USA) or goat anti-rabbit IgG (Santa Cruz Biotechnology) for 1 h at room temperature. After washing with TBST, the peroxidase activity on the membranes was detected by a chemiluminescence method using an ECL Plus kit (Amersham Pharmacia Biotech, Buckinghamshire, UK) and exposed to X-ray films (Kodak, Rochester, USA). The amounts of Cyt c protein were quantified by scanning X-ray films by Densitography (Atto, Tokyo, Japan).

Induction of experimental cryptorchidism

Experimental cryptorchidism was induced in mice as described previously [32]. A group of mature male mice were made cryptorchid surgically under sodium barbital anesthesia (4 mg/kg body weight). One testis of each animal was translocated and sutured to the lateral abdominal wall via the fat pad. The other testis was sham operated and used as a control. Care was taken not to injure blood vessels or the epididymis. The animals were killed at appropriate days after cryptorchidism. Mice were used for analyses only when the testes were located abdominally at post mortem and were atrophic.

Histological examination and detection of DNA fragmentation in situ

A half of each testis was fixed in Bouin solution for 16 h at 4°C and embedded in paraffin. Four micro meter thick sections were mounted on silan-coated glass slides, deparaffinized, and hydrated. They were digested with 20 μg/ml of proteinase K for 15 min at room temperature. Endogenous peroxidase was inactivated by incubation in a 3% hydrogen peroxide solution for 5 min at room temperature. A histological examination was performed on hematoxylin and eosin (HE)-stained sections. Apoptotic nuclei in tissue sections were identified by a terminal deoxynucleotidyl transferase-mediated deoxyuridine triphosphate nick end labeling (TUNEL) technique using an *in situ* apoptosis detection kit (Takara, Kyoto, Japan) according to the manufacture's instructions. Photographs were taken with a digital camera under microscopy (Olympus BX50, Tokyo, Japan). Cross sections of two hundred round, transversely cut seminiferous tubules from eight testes from each group were examined. The number of TUNEL-positive nuclei per tubule was calculated and are expressed as the mean ± SEM for each group, as described previously [28].

Statistical analysis

Statistical analyses of the data were carried out using the Mann–Whitney *U*-test. $P < 0.05$ was considered to be significant.

Results

Effects of experimental cryptorchidism on SOD1 KO and WT mice

To examine the possible involvement of ROS in spermatogenic cell damage *in vivo*, we employed SOD1-KO mice. If superoxide is generated during heat stress and is responsible for the damage, an enhanced testicular impairment would be expected in the SOD1-KO mice. As a result, although the testicular weight of SOD1-KO mice was not altered from that of WT mice at an early stage, it became significantly less at the late stage of cryptorchidism (Figure 1). Histological analysis indicated that vacuolar degeneration was more sever in the SOD1-KO than the WT mice (Figure 2). When DNA fragmentation was detected *in situ* using the TUNEL assay, more positive signals were found for SOD1-KO than for WT mice. The number of TUNEL-positive cells that were generally regarded as apoptotic cells was the highest at day 7 and then

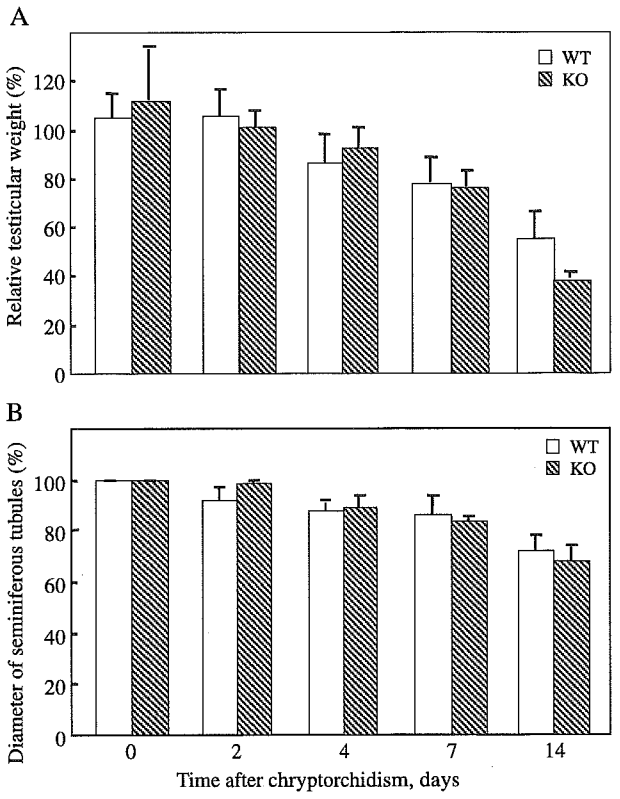

Figure 1. Changes in testicular weight of wild-type and SOD1-KO mice during experimental cryptorchidism. (A) After the induction of experimental cryptorchidism, testicular weight was measured over a 2-week period. Relative testicular weight to sham-operated control were shown (%). (B) Diameter of seminiferous tubules were also measured. (Numbers of animals were 3–6, except for 2 of 0-day control KO mice).

decreased (Figure 3). At day 14, positive signals were higher in the WT than the SOD1-KO mice. This can be explained by the exhaustion of spermatogenic cells in SOD1-KO mice at an early stage, due to their enhanced vulnerability. Thus, cell death by cryptorchidism is accelerated in SOD1-KO mice.

Expression of antioxidative/redox enzymes in cryptorchid mice

We then examined the levels of proteins that function as antioxidative and redox enzymesn by immunoblotting (Figure 4). The levels of CuZnSOD were decreased slightly during cryptorchidism in WT mice while no CuZnSOD protein was detected in SOD1-KO mice. The levels of MnSOD, a mitochondrial SOD isoform, and Prx1, a thioredoxin-dependent peroxidase 1, were not altered significantly in either type of mice.

Effects of high temperature on cultured spermatogenic cells from SOD1-KO and WT mice

To gain an insight into the high vulnerability of SOD1-KO mice in cryptorchidism, spermatogenic cells were isolated from SOD1-KO and WT mice and cultivated at 32.5 and 37°C. While incubation, even at 32.5°C, slowly decreased the number of the cells isolated from WT mice, the number decreased at an accelerated rate in the cells from SOD1-KO mice (Figure 5A). The cells from SOD1-KO mice decreased more rapidly than those from WT mice when incubated at 37°C. The incidence of cell death was significantly higher in SOD1-KO than WT mice at day 3. Thus, a deficiency of SOD1 appears to be related to the high vulnerability of spermatogenic cells under the culture conditions used here. Spermatogenic cells were partially protected against heat by tiron, a superoxide-scavenging compound (Figure 5B). These data farther support the conclusion that ROS is involved in heat stress-induced cell damage.

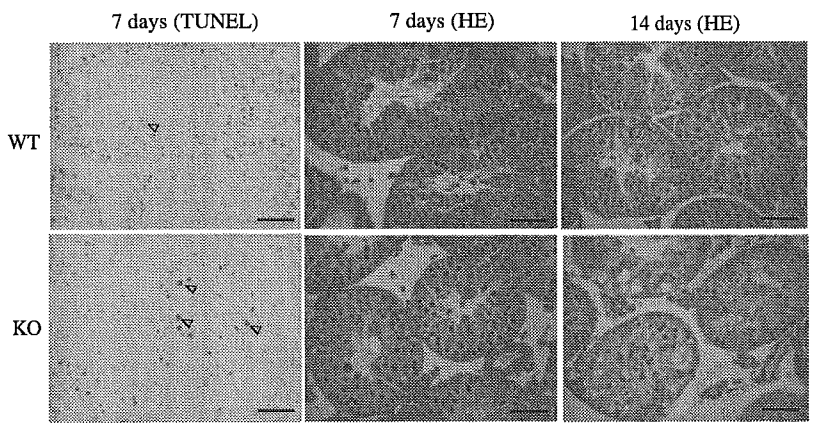

Figure 2. In situ detection of DNA fragmentation in WT and SOD1-KO mice. After the induction of experimental cryptorchidism, tissue sections were prepared from the isolated testes. A histological analysis was performed on HE-stained sections. Localization of apoptotic cells was detected by a TUNEL assay of a paraffin-embedded section from WT and SOD1-KO mice testes. Typical data at 7 and 14 days after cryptorchidism from a series of experiments were shown. Arrowheads; TUNEL-positive cells. (bar = 100 μm)

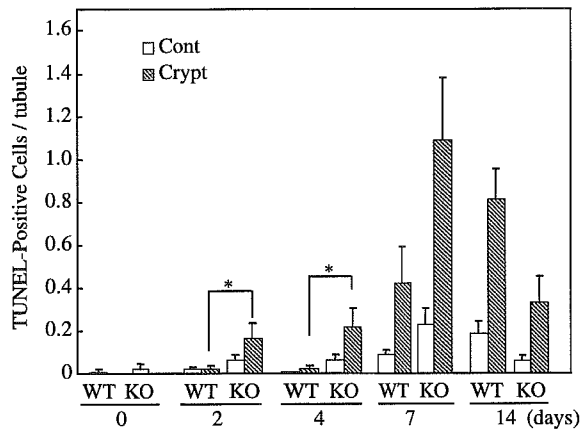

Figure 3. Comparison of the number of apoptotic cells between SOD1-KO and WT mice during experimental cryptorchidism. The TUNEL assay was performed for both SOD1-KO and WT mice at each time point. The number of TUNEL-positive cells per seminiferous tubules was counted for each mouse. (Numbers of animals were 3–8, *; $P < 0.05$ versus WT at the same time point).

Susceptibility of testicular cells to ROS

We examined the differential sensitivity of spermatogenic cells from Sertoli cells to ROS, the levels of which are assumed to be augmented by heat stress of the testes. Both spermatogenic cells and Sertoli cells were isolated from rats and cultivated separately at the normal testicular temperature of 32.5°C. These cells were incubated with 2 mM hypoxanthine and varying concentrations of xanthine oxidase, a ROS generator, that produces primarily superoxide, for 1 h. Cytosolic fractions were isolated and subjected to immunoblotting using the anti-Cyt c antibody (Figure 6). Cyt c was released into the cytoplasm from mitochondria in spermatogenic cells in a xanthine oxidase dose-dependent manner, while no change was observed in Sertoli cells. Thus, spermatogenic cells were found to be more susceptible to ROS than Sertoli cells. This profile of the two types of cells is consistent with the heat-induced Cyt c release in culture [28].

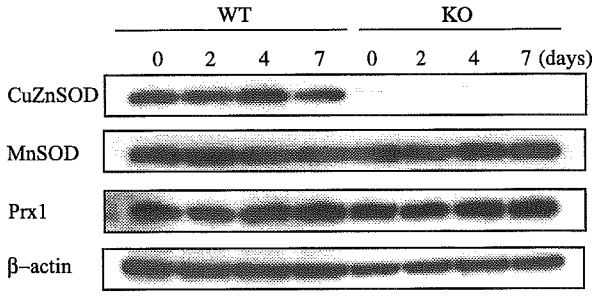

Figure 4. Immunoblot analysis of some antioxidative/redox proteins. Soluble proteins were prepared from testes at 0, 2, 4 and 7 days after the induction of cryptorchidism and subjected to immunoblot analysis using antibodies against SOD1, SOD2, Prx1, GR, and β-actin. Typical data of several experiments were shown.

Suppression of cytochrome c release from mitochondria by Tiron

We next determined whether or not superoxide was actually involved in the release of Cyt c into the cytosol from mitochondria in spermatogenic cells. Cultivated spermatogenic cells were exposed to a temperature at 42°C for 1 h. A longer exposure than that used to induce heat stress in testis is required in a culture system because the temperature of the medium is elevated gradually in a CO_2 incubator compared with the use of hot water bath. Tiron at a concentration 10 μM significantly suppressed the release of Cyt c from mitochondria (Figure 7). This suggests that superoxide, generated during hyperthermic conditions, is responsible for the release of cytochrome c.

Discussion

Data is presented that supports the involvement of ROS in heat-induced spermatogenic cell damage in *ex vivo* and *in vivo* heat stress models. Spermatogenic cells in primary culture appeared to be highly susceptible to ROS and died (Figure 6). Since tiron, a superoxide scavenger, suppressed the release of cytochrome c from mitochondria (Figure 7), an elevation in superoxide levels under these conditions and its involvement in the cytotoxic process can be expected. The generation of ROS will be augmented in response to an elevated metabolism accompanied by oxygen consumption. The contents of the redox enzymes glutathione reductase and aldo-keto reductase, which function in the detoxification of ROS and resulting carbonyl compounds, are much lower in spermatogenic cells than in Sertoli cells [29,33,34]. If ROS are a direct cause of cell death, the higher susceptibility of spermatogenic cells to elevated temperature can be attributed to the lower levels of these antioxidative/redox enzymes.

Although we did not observe significant elevation of ROS in cultured cells under heat-stress (data not shown), we indirectly demonstrated involvement of ROS in spermatogenic cell death. The use of SOD1-KO mice supports the view that ROS are mediators of cytotoxicity. The expression of various genes, including some antioxidative enzyme genes, is altered in response to stimuli in rat testes and, hence, can be regarded as stress responsible genes [35]. A decrease in the levels of SOD1 activity and mRNA levels have been reported in experimental cryptorchid testes of genetically normal animals [36,37]. We have also found that the processing of Prx4, a multifunctional redox protein with thioredoxin-dependent peroxidase activity, presumably plays a role in the spermatogenic process [38,39] and is altered in the cryptorchid testes of mice [40]. However, the levels of MnSOD and Px1 were

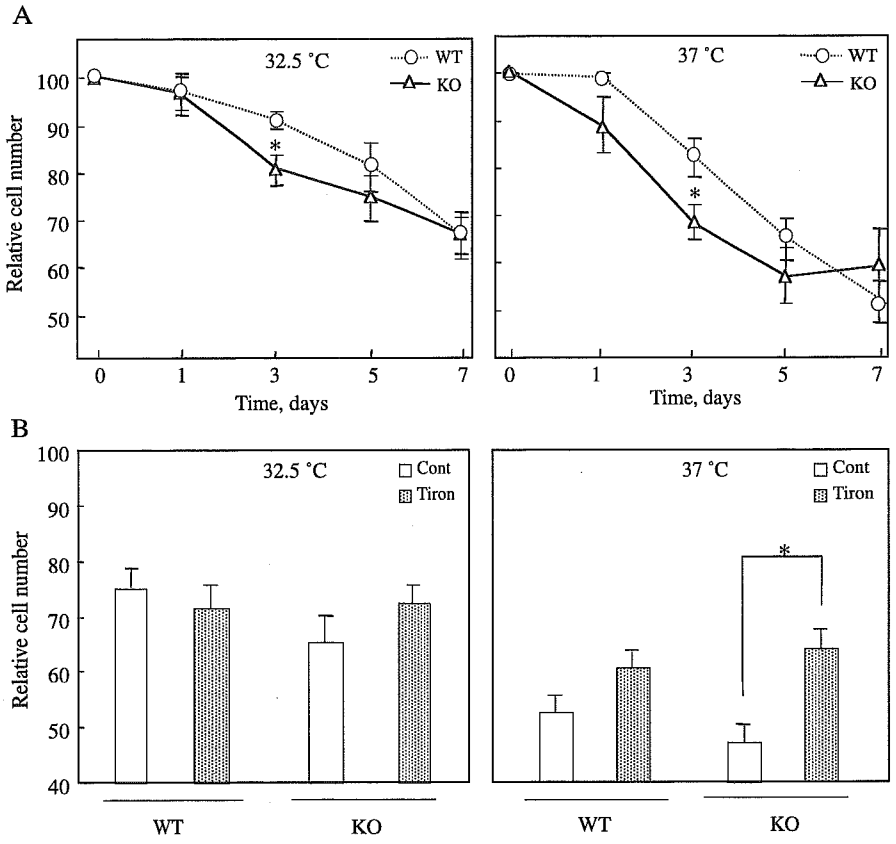

Figure 5. Comparison of the effects of heat stress on the vulnerability of spermatogenic cells between SOD1-KO and WT mice in culture. (A) After isolation from testes, the cultured cells were incubated at either 32.5 or 37°C for up to 7 days. ($n = 3$, *; $P < 0.05$ versus WT at the same time point). (B) Tiron was added to 10 μM into culture media at day 0 and further incubated at 32.5 or 37°C for 3 days. Number of cells was counted at each time point. ($n = 3$, *; $P < 0.05$ versus control).

unchanged during this period of cryptorchidism (Figure 4), suggesting a minimal role of these antioxidative/redox proteins in the heat-induced damage of spermatogenic cells.

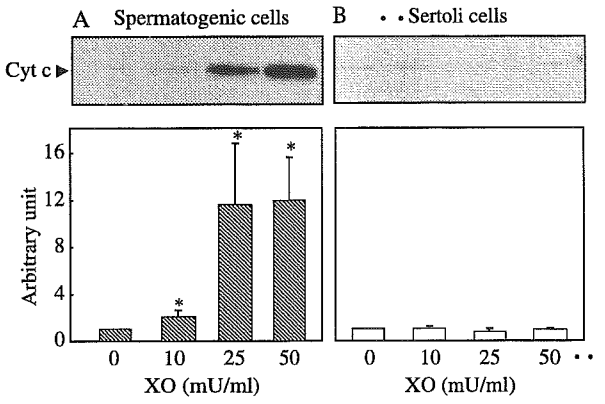

Figure 6. Effects of ROS produced from hypoxanthine/xanthine oxidase on the release of cytochrome c in spermatogenic and Sertoli cells. Spermatogenic cells (A) and Sertoli cells (B) were isolated from rat testis and cultivated at 32.5°C. After incubation with 2 mM hypoxanthine and varying concentrations of xanthine oxidase for 1 h, the cytosolic fraction was prepared from the cells. Proteins were analyzed by immunoblotting with an anti-cytochrome c monoclonal antibody. Cytochrome c bands on blots were quantified by densitometry. ($n = 3$, *; $P < 0.05$ versus without XO).

An elevation in lipid peroxidation products has been reported in experimental cryptorchidism in the case of mouse and rat testes [16]. Since testes are rich in unsaturated fatty acids, which are essential for sperm motility and highly susceptible to peroxidation, protection against oxidative modification by phospholipid hydroperoxide glutathione peroxidase (PhGPx) is of major importance [41]. Dysfunction in PhGPx and male infertility are highly correlated [42,43]. Thus, protection against oxidative stress, including lipid peroxidation, appears to be a central mechanism in the maintenance of male fertility. Although a linkage analysis between male infertility and genetic variations of PhGPx has been systematically carried out in men, the results were inconclusive [44]. Similarly, no correlation between a genetic defect of SOD1 and infertility has been reported. Further study will be required to clarify this point.

Isolated spermatogenic cells spontaneously die, even at the scrotum temperature 32.5°C, while Sertoli cells grow. A lack of support by Sertoli cells would be a major cause for this cell death. In addition, the hyperoxic environment in a CO_2 incubator, compared to the testis, could also be another factor. Hyperoxic conditions may enhance the production of ROS in cells during the metabolic process and impair cell

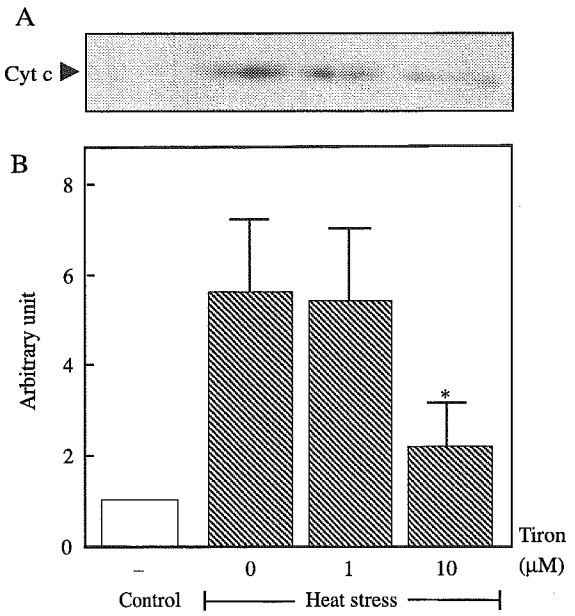

Figure 7. Effects of tiron on the heat stress-induced release of cytochrome c from spermatogenic cells. Spermatogenic cells were incubated at 42°C for 1 h in the presence or absence of tiron. After 30 min, the cytosolic fraction was prepared from the cells. Proteins were analyzed by immunoblotting with an anti-cytochrome c monoclonal antibody. Cytochrome c bands on blots were quantified by a densitometry. ($n = 3$, *; $P < 0.05$ versus the heat-stress group without tiron).

viability. An increase in ROS production by heat stress has been reported in spermatogenic cell cultures [15]. The origin of ROS may be xanthine oxidase activity because the use of allopurinol, a xanthine oxidase inhibitor, resulted in a lower number of TUNEL-positive cells and ameliorated spermatogenic cell damage in cryptorchid testes of rats [45]. Although vulnerable cells, such as pachytene spermatocytes and early spermatids die quickly, the remaining cells appear to be rather resistant [7]. This explains why the cell number under cultural conditions was significantly lower at day 3 only in SOD1-KO, compared to WT mice (Figure 5).

There is another possible explanation for the involvement of ROS in spermatogenic cell death by heat stress. Even a short period of heat exposure, e.g. 43°C for 15 min, triggers damage in spermatogenic cells without any apparent increase in ROS levels. This suggests that ROS generated under these conditions may function as a type of signal rather than a direct oxidant. In the intrinsic apoptotic pathway, ROS typically triggers the release of cytochrome c from mitochondria into the cytosol and leads to the activation of the caspase cascade [46]. ROS is known to modulate the function of signaling molecules, such as protein-tyrosine phosphatase [47] and G proteins [48]. Since an SOD1 deficiency would prolong the ROS signal, the acceleration in the testicular damage of SOD1-KO mice by heat stress might be induced by the production of a sustained signal for cell death.

In conclusion, since SOD1 deficiency accelerated testicular impairment and tiron suppressed cytotoxicity under heat stress, ROS are likely cytotoxic mediators in spermatogenic cells during heat stress. There are two possible pathways for the involvement of ROS. One is the oxidation of specific important molecules, such as unsaturated fatty acids [16], resulting in the direct impairment of cells. The other is signal mediation and the activation of the death pathway in response to heat stress. Even weak signal that is not harmful for somatic cells would cause a detrimental consequence in spermatogenic cells because of quality control of sperm. Further analysis of death signaling pathway in germ cells by heat stress would clarify this issue.

Acknowledgements

We thank Ms Masako Seki for maintenance of laboratory equipments and secretarial services. This work was supported, in part, by Grant-in-Aid for Scientific Research (C) (No. 16590238), JSPS Fellowship (No. 13007321), and 21st Century COE Program from Japan Society for the Promotion of Science (JSPS).

References

[1] Frankenhuis MT, Wensing CJ. Induction of spermatogenesis in the naturally cryptorchid pig. Fertil Steril 1979;31:428–433.

[2] Lue YH, Sinha Hikim AP, Swerdloff RS, Im P, Taing KS, Bui T, Leung A, Wang C. Single exposure to heat induces stage-specific germ cell apoptosis in rats: Role of intratesticular testosterone (T) on stage specificity. Endocrinology 1999; 140:1709–1717.

[3] Miura M, Sasagawa I, Suzuki Y, Nakada T, Fujii J. Apoptosis and expression of apoptosis related genes in the mouse testis following heat exposure. Fertil Steril 2002;77:787–793.

[4] Chowdhury AK, Steinberger E. Early changes in the germinal pithelium of rat testes following exposure to heat. J Reprod Fertil 1970;22:205–212.

[5] Mieusset R, Bujan L, Mondinat C, Mansat A, Pontonnier F, Grandjean H. Association of scrotal hyperthermia with impaired spermatogenesis in infertile men. Fertil Steril 1987;48:1006–1011.

[6] Rommerts FF, de Jong FH, Grootegoed JA, van der Molen HJ. Metabolic changes in testicular cells from rats after long-tern exposure to 37°C *in vivo* or *in vitro*. J Endocrinol 1980;85: 471–479.

[7] Setchell BP. The Parkes lecture. Heat and the testis. J Reprod Fertil. 1998;114:179–194.

[8] Shikone T, Billig H, Hsueh AJ. Experimentally induced cryptorchidism increases apoptosis in rat testis. Biol Reprod 1994;51:865–872.

[9] Yin Y, Hawkins KL, DeWolf WC, Morgentaler A. Heat stress causes testicular germ cell apoptosis in adult mice. J Androl 1997;18:159–165.

[10] Yin Y, DeWolf WC, Morgentaler A. Experimental cryptorchidism induces testicular germ cell apoptosis by p53-dependent

and-independent pathways in mice. Biol Reprod 1998;58: 492–496.

[11] Yin Y, Stahl BC, DeWolf WC, Morgentaler A. P53 and Fas are sequential mechanisms of testicular germ cell apoptosis. J Androl 2002;23:64–70.

[12] Yamamoto CM, Sinha Hikim AP, Huynh PN, Shapiro B, Lue Y, Salameh WA, Wang C, Swerdloff RS. Redistribution of bax is an early step in an apoptotic pathway leading to germ cell death in rats, triggered by mild testicular hyperthermia. Biol Reprod 2000;63:1683–1690.

[13] Yan W, Samson M, Jegou B, Toppari J. Bcl-w forms complexes with Bax and Bak, and elevated ratios of Bax/Bcl-w and Bak/Bcl-w correspond to spermatogonial and spermatocyte apoptosis in the testis. Mol Endocrinol 2000;14:682–699.

[14] Sinha Hikim AP, Lue Y, Yamamoto CM, Vera Y, Rodriguez S, Yen PH, Soeng K, Wang C, Swerdoff RS. Key apoptotic pathways for heat-induced programmed germ cell death in the testis. Endocrinology 2003;144:3167–3175.

[15] Ikeda M, Kodama H, Fukuda J, Shimizu Y, Murata M, Kumagai J, Tanaka T. Role of radical oxygen species in rat testicular germ cell apoptosis induced by heat stress. Biol Reprod 1999;61:393–399.

[16] Peltola V, Huhtaniemi I, Ahotupa M. Abdominal position of the rat testis is associated with high level of lipid peroxidation. Biol Reprod 1995;53:1146–1150.

[17] Fridovich I. Superoxide radical and superoxide dismutases. Annu Rev Biochem 1995;64:97–112.

[18] Mruk DD, Silvestrini B, Mo MY, Cheng CY. Antioxidant superoxide dismutase—a review: Its function, regulation in the testis, and role in male fertility. Contraception 2002; 65:305–311.

[19] Fujii J, Iuchi Y, Matsuki S, Ishii T. Cooperative function of antioxidant and redox systems against oxidative stress in male reproductive tissues. Asian J Androl 2003;5:231–242.

[20] Suzuki K, Ohno H, Oh-ishi S, Kizaki T, Ookawara T, Fujii J, Radak Z, Taniguchi N. Superoxide dismutases in exercise and disease. In: Sen CK, Packer L, Hanninen O, editors. Handbook of Oxidants and Antioxidants in Exercise. Amsterdam: Elsevier Science; 2000. p 243–295.

[21] Reaume AG, Elliott JL, Hoffman EK, Kowall NW, Ferrante RJ, Jr., Siwek DF, Wilcox HM, Flood DG, Beal MF, Brown, RH, Scott RW, Snider WD. Motor neurons in Cu/Zn superoxide dismutase-deficient mice develop normally but exhibit enhanced cell death after axonal injury. Nat Genet 1996;3:43–47.

[22] Ho YS, Gargano M, Cao J, Bronson RT, Heimler I, Hutz RJ. Reduced fertility in female mice lacking copper–zinc superoxide dismutase. J Biol Chem 1998;273:7765–7769.

[23] Matzuk MM, Dionne L, Guo Q, Kumar TR, Lebovitz RM. Ovarian function in superoxide dismutase 1 and 2 knockout mice. Endocrinology 1998;139:4008–4011.

[24] Shefner JM, Reaume AG, Flood DG, Scott RW, Kowall NW, Ferrante RJ, Siwek DF, Upton-Rice M, Brown RH, Jr. Mice lacking cytosolic copper/zinc superoxide dismutase display a distinctive motor axonopathy. Neurology 1999; 53:1239–1246.

[25] Yoshida T, Maulik N, Engelman RM, Ho YS, Das DK. Targeted disruption of the mouse Sod 1 gene makes the hearts vulnerable to ischemic reperfusion injury. Circ Res 2000;86: 264–269.

[26] Li Y, Huang TT, Carlson EJ, Melov S, Ursell PC, Olson JL, Noble LJ, Yoshimura MP, Berger C, Chan PH, Wallace DC, Epstein CJ. Dilated cardiomyopathy and neonatal lethality in mutant mice lacking manganese superoxide dismutase. Nat Genet 1995;11:376–381.

[27] Raineri I, Carlson EJ, Gacayan R, Carra S, Oberley TD, Huang TT, Epstein CJ. Strain-dependent high-level expression of a transgene for manganese superoxide dismutase is associated with growth retardation and decreased fertility. Free Radic Biol Med 2001;31:1018–1030.

[28] Matsuki S, Iuchi Y, Ikeda Y, Sasagawa I, Tomita Y, Fujii J. Suppression of cytochrome c release and apoptosis in testes with heat stress by minocycline. Biochem Biophys Res Commun 2003;312:843–849.

[29] Kaneko T, Iuchi Y, Kobayashi T, Fujii T, Saito H, Kurachi H, Fujii J. Expression of glutathione reductase in the male reproductive system of rats supports the enzymatic basis of glutathione function in spermatogenesis. Eur J Biochem 2002;269:1570–1578.

[30] Suzuki K, Tatsumi H, Satoh S, Senda T, Nakata T, Fujii J, Taniguchi N. Manganese-superoxide dismutase in endothelial cells: Localization and mechanism of induction. Am J Physiol 1993;265:H1173–H1178.

[31] Okado-Matsumoto A, Matsumoto A, Fujii J, Taniguchi N. Peroxiredoxin IV is a secretable protein with heparin-binding properties under reduced conditions. J Biochem 2000; 127:493–501.

[32] Iuchi Y, Kaneko T, Matsuki S, Sasagawa I, Fujii J. Concerted changes in the YB2/RYB-a protein and protamine 2 messenger RNA in the mouse testis under heat stress. Biol Reprod 2003;68:129–135.

[33] Iuchi Y, Kaneko T, Matsuki S, Ishii T, Ikeda Y, Uchida K, Fujii J. Carbonyl stress and detoxification ability in the male genital tract and testis of rats. Histochem. Cell Biol 2004; 121:123–130.

[34] Kobayashi T, Kaneko T, Iuchi Y, Matsuki S, Takahashi M, Sasagawa I, Nakada T, Fujii J. Localization and physiological implication of aldose reductase and sorbitol dehydrogenase in reproductive tracts and spermatozoa of male rats. J Androl 2002;23:674–683.

[35] Aguilar-Mahecha A, Hales BF, Robaire B. Expression of stress response gene in germ cells during spermatogenesis. Biol Rerod 2001;61:119–127.

[36] Ahotupa M, Huhtaniemi I. Impaired detoxification of reactive oxygen and consequent oxidative stress in experimentally cryptorchid rat testis. Biol Reprod 1992;46:1114–1118.

[37] Zini A, Schlegel PN. Cu/Zn superoxide dismutase, catalase and glutathione peroxidase mRNA expression in the rat testis after surgical cryptorchidism and efferent duct ligation. J Urol 1997;158:659–663.

[38] Sasagawa I, Matsuki S, Suzuki Y, Iuchi Y, Tohya K, Kimura M, Nakada T, Fujii J. Possible involvement of the membrane-bound form of peroxiredoxin 4 in acrosome formation during spermiogenesis of rats. Eur J Biochem 2001;268:3053–3061.

[39] Fujii J, Ikeda Y. Peroxiredoxins in mammals: recent advances of multifunctional redox proteins. Redox Rep 2002;7:123–130.

[40] Matsuki S, Sasagawa I, Iuchi Y, Fujii J. Impaired expression of peroxiredoxin 4 in damaged testes by artificial cryptorchidism. Redox Rep 2002;7:276–278.

[41] Imai H, Nakagawa Y. Biological significance of phospholipid hydroperoxide glutathione peroxidase (PHGPx, GPx4) in mammalian cells. Free Radic Biol Med 2003;34:145–169.

[42] Imai H, Suzuki K, Ishizaka K, Ichinose S, Oshima H, Okayasu I, Emoto K, Umeda M, Nakagawa Y. Failure of the expression of phospholipid hydroperoxide glutathione peroxidase in the spermatozoa of human infertile males. Biol Reprod 2001;64:674–683.

[43] Foresta C, Flohe L, Garolla A, Roveri A, Ursini F, Maiorino M. Male fertility is linked to the selenoprotein phospholipid hydroperoxide glutathione peroxidase. Biol Reprod 2002; 67:967–971.

[44] Maiorino M, Bosello V, Ursini F, Foresta C, Garolla A, Scapin M, Sztajer H, Flohe L. Genetic variations of gpx-4 and male infertility in humans. Biol Reprod 2003;68:1134–1141.

[45] Kumagai A, Kodama H, Kumagai J, Fukuda J, Kawamura K, Tanikawa H, Sato N, Tanaka T. Xanthine oxidase inhibitors

suppress testicular germ cell apoptosis induced by experimental cryptorchidism. Mol Hum Reprod 2002;8:118–123.

[46] Hengartner MO. The biochemistry of apoptosis. Nature 2000;407:770–776.

[47] Lee SR, Kwon KS, Kim SR, Rhee SG. Reversible inactivation of protein-tyrosine phosphatase 1B in A431 cells stimulated with epidermal growth factor. J Biol Chem 1998; 273: 15366–15372.

[48] Nishida M, Schey KL, Takagahara S, Kontani K, Katada T, Urano Y, Nagano T, Nagao T, Kurose H. Activation mechanism of Gi and Go by reactive oxygen species. J Biol Chem 2002;277:9036–9042.

Dysregulation of TGF-β1 receptor activation leads to abnormal lung development and emphysema-like phenotype in core fucose-deficient mice

Xiangchun Wang[a,b], Shinya Inoue[a,b,c], Jianguo Gu[a], Eiji Miyoshi[a], Katsuhisa Noda[a], Wenzhe Li[d], Yoko Mizuno-Horikawa[a], Miyako Nakano[a], Michio Asahi[a], Motoko Takahashi[a,e], Naofumi Uozumi[a], Shinji Ihara[a], Seung Ho Lee[a], Yoshitaka Ikeda[a,e], Yukihiro Yamaguchi[a,f], Yoshiya Aze[g], Yoshiaki Tomiyama[c], Junichi Fujii[a,h], Keiichiro Suzuki[a,f], Akihiro Kondo[d], Steven D. Shapiro[i], Carlos Lopez-Otin[j], Tomoyuki Kuwaki[k], Masaru Okabe[l], Koichi Honke[a,m], and Naoyuki Taniguchi[a,n]

Departments of [a]Biochemistry, [c]Internal Medicine and Molecular Science, and [d]Glycotherapeutics, Osaka University Graduate School of Medicine, Osaka 565-0871, Japan; [e]Department of Cell Biology, Saga University School of Medicine, Saga 809-8501, Japan; [f]Department of Biochemistry, Hyogo College of Medicine, Hyogo 663-8501, Japan; [g]Fukui Safety Institute, Ono Pharmaceutical Co., Fukui 913-8538, Japan; [h]Department of Biochemistry, Yamagata University School of Medicine, Yamagata 990-9585, Japan; [i]Department of Medicine, Section of Pulmonary and Critical Care Medicine, Brigham and Women's Hospital, Boston, MA 02115; [j]Departamento de Bioquimica y Biologia Molecular, Instituto Universitario de Oncologia, Universidad de Oviedo, 33006 Oviedo, Spain; [k]Department of Molecular and Integrative Physiology, Graduate School of Medicine, Chiba University, Chiba 260-8670, Japan; [l]Department of Experimental Genome Research, Genome Information Research Center, Osaka University, Osaka 565-0871, Japan; and [m]Department of Molecular Genetics, Kochi University Medical School, Kochi 783-8505, Japan

Communicated by David H. MacLennan, University of Toronto, Toronto, ON, Canada, August 24, 2005 (received for review August 2, 2005)

The core fucosylation (α1,6-fucosylation) of glycoproteins is widely distributed in mammalian tissues, and is altered under pathological conditions. To investigate physiological functions of the core fucose, we generated α1,6-fucosyltransferase (*Fut8*)-null mice and found that disruption of *Fut8* induces severe growth retardation and death during postnatal development. Histopathological analysis revealed that *Fut8*$^{-/-}$ mice showed emphysema-like changes in the lung, verified by a physiological compliance analysis. Biochemical studies indicated that lungs from *Fut8*$^{-/-}$ mice exhibit a marked overexpression of matrix metalloproteinases (MMPs), such as MMP-12 and MMP-13, highly associated with lung-destructive phenotypes, and a down-regulation of extracellular matrix (ECM) proteins such as elastin, as well as retarded alveolar epithelia cell differentiation. These changes should be consistent with a deficiency in TGF-β1 signaling, a pleiotropic factor that controls ECM homeostasis by down-regulating MMP expression and inducing ECM protein components. In fact, *Fut8*$^{-/-}$ mice have a marked dysregulation of TGF-β1 receptor activation and signaling, as assessed by TGF-β1 binding assays and Smad2 phosphorylation analysis. We also show that these TGF-β1 receptor defects found in *Fut8*$^{-/-}$ cells can be rescued by reintroducing *Fut8* into *Fut8*$^{-/-}$ cells. Furthermore, exogenous TGF-β1 potentially rescued emphysema-like phenotype and concomitantly reduced MMP expression in *Fut8*$^{-/-}$ lung. We propose that the lack of core fucosylation of TGF-β1 receptors is crucial for a developmental and progressive/destructive emphysema, suggesting that perturbation of this function could underlie certain cases of human emphysema.

fucosylation | glycobiology | matrix metalloproteinase

The physiological importance of fucose modifications on proteins has been highlighted recently by the description of human congenital disorders of glycosylation (CDG). The disease CDG-IIc is due to lack of the GDP-fucose transporter activity (1, 2). α1,2-, α1,3-, α1,4-, and α1,6-fucosylations have been described; α1,6-fucose is found linked to the Asn-linked GlcNAc in the *N*-glycan core. All of these fucosylations are terminal capping reactions, and the fucose residues have no substituent. In contrast, O-fucosylation, in which fucose is attached directly to a serine or threonine residue in a particular protein context such as an EGF repeat, undergoes the elongation of the oligosaccharide into a tetrasaccharide (NeuAcα2–3/6Galβ1–4GlcNAcβ1–3Fuc-Ser/Thr), in which Fringe has been found to be the *N*-acetylglucosaminyltransferase acting on O-linked fucose of the Notch receptor (3). Because Notch receptors play key roles in numerous developmental events, several features of the phenotype in CDG-IIc could be explained by defects in Notch function. However, Sturla *et al.* (4, 5) reported that reduced fucosylation is mainly confined to terminal fucosylation of *N*-glycans, and that protein O-fucosylation levels such as those that occur in Notch are unaffected in CDG-IIc; therefore, we speculate that core fucosylation may be responsible for the phenotype of CDG-IIc.

GDP-L-Fuc:*N*-acetyl-β-D-glucosaminide α1,6-fucosyltransferase (Fut8, EC 2.4.1.152) catalyzes the transfer of a fucose residue from GDP-fucose to position 6 of the innermost GlcNAc residue of hybrid and complex types of N-linked oligosaccharides on glycoproteins (6). Core Fut8 is the only core FucT in mammals, but there are core α1,3-Fuc residues in plants, insects, and probably other species. The *Fut8* gene is expressed in most rat organs with a relatively high level of expression in brain and small intestine (7). In good agreement with the *Fut8* gene expression, α1,6-fucosylated glycoproteins are widely distributed in mammalian tissues (8). Furthermore, the expression of Fut8 and the extent of core fucosylation are altered under pathological conditions such as hepatocellular carcinoma and liver cirrhosis (8, 9).

The molecular cloning of the *Fut8* gene (10) enabled us to manipulate it and to remodel the *N*-glycans in animal models. Overexpression of the *Fut8* gene caused steatosis in the liver and kidney due to a decreased lysosomal acid lipase activity accompanied by its over-fucosylation (11). Recently, it was reported that the core fucose-deficient IgG1 (produced in a fucose-deficient Chinese hamster ovary cell line) showed improved binding to FcγRIIIA. As a consequence, antibody-dependent cellular cytotoxicity activity mediated by their interaction was enhanced (12, 13). These findings strongly suggested that core fucosylation of *N*-glycans modifies the function of the glycoproteins.

To define the physiological roles of a particular glycosylation, gene targeting technology to disrupt the relevant glycosyltrans-

Freely available online through the PNAS open access option.

Abbreviations: ECM, extracellular matrix; MMP, matrix metalloproteinase; PA, 2-aminopyridine.

See Commentary on page 15721.

[b]X.W. and S. Inoue contributed equally to this work.

[n]To whom correspondence should be addressed at: Department of Biochemistry, Osaka University Graduate School of Medicine, 2-2 Yamadaoka, Suita, Osaka 565-0871, Japan. E-mail: proftani@biochem.med.osaka-u.ac.jp.

ferase gene function is considered as the best approach currently available. In fact, accumulating evidence on gene targeting for glycosyltransferases has elucidated a variety of novel functions of carbohydrates and provided new insights into their roles *in vivo* (14). Here we report the generation of *Fut8*-null mice and describe critical roles of core fucosylation *in vivo*.

Materials and Methods

Gene Targeting. A part of the mouse *Fut8* gene spanning 13.9 kb, which includes the exon containing the translation-initiation site, was isolated by screening a mouse 129SvJ λ genomic library (Stratagene), using a SacI–SacI fragment of porcine *Fut8* cDNA (nt −39 to 373) (10) as a probe. A targeting vector was constructed by replacing the 184-bp SacI–HindIII fragment containing the translation-initiation site with a 4.9-kb SacI–SalI fragment of the plasmid pGT1.8IresBgeo (15) that contains an internal ribosome entry site (*IRES*)-*LacZ*-*Neo*^{r}- polyadenylation signal (*pA*) cassette, flanked with a 1.5-kb XhoI–NotI fragment of the plasmid pMC1DTpA (16), which encodes diphtheria toxin A chain (*DT-A*) for negative screening (see Fig. 4, which is published as supporting information on the PNAS web site). The targeting vector was transfected into D3 embryonic stem cells, and clones were selected with G418. Southern blot analysis of selected clones with 5′ (*A*) and 3′ (*B*) probes (Fig. 4) revealed that 1.2% (4 of 343) of the embryonic stem clones had undergone correct homologous recombination. Targeted cell clones were then injected into blastocysts from B6C3F1 mice, which are F_1 mice resulting from the intercross of female C57BL/6 and male C3H mice. Germ-line transmission of the mutant allele was achieved from male chimeras derived from two independent embryonic stem cell clones.

Oligosaccharide Structural Analyses of the Mouse Lungs. N-linked oligosaccharides of lung were liberated by hydrazinolysis at 100°C for 10 h and then re-N-acetylated. The reducing ends of the oligosaccharides were labeled with 2-aminopyridine (PA) as described in ref. 17. PA-oligosaccharides were subjected to HPLC analysis and further to liquid chromatography–electrospray ionization–MS analysis, which was performed on an HCT ion trap mass spectrometer (Bruker Daltonics, Bremen, Germany) equipped with an electrospray source working in positive ion mode.

Measurement of Lung Compliance and Ventilation. Lung compliance was measured by drawing static air pressure–volume relations in urethane-anesthetized (1.5 g/kg) mice tracheotomized with polyethylene tubing (O.D. = 0.8 mm). Total lung capacity was defined as the lung volume of full inflation as judged by visual inspection of the lung that fully occupied the chest cavity. Any obvious, continual decrease in the pressure was evidence of a leaking lung, which was then discarded. The lung volumes at each measured point were expressed as a percentage of the total lung capacity. Ventilation was measured by whole-body plethysmography in unanesthetized freely moving mice as reported in ref. 18.

Establishment of Embryonic Fibroblasts. For preparation of embryonic fibroblasts, a whole mouse embryo at 18.5 days postcoitus was dissected, and the head and all internal organs were removed. The carcasses were minced, incubated in PBS (−) containing 0.05% trypsin, 0.53 mM EDTA, and 40 μg/ml DNase at 37°C for 30 min with stirring three times, and then cells were plated on a 100-mm dish in DMEM supplemented with 10% FCS and incubated at 37°C in humidified air containing 5% CO_2. To obtain immortal cells, Zeocine-resistant vector (pcDNA3.1) containing the SV40 gene was introduced to these primary embryonic fibroblasts. Transfectants were screened in the presence of 400 μg/ml Zeocine, and SW (wild-type cells immortalized with SV40 gene) and SK (knockout cells immortalized with SV40 gene) immortal cells were established from *Fut8*$^{+/+}$ and *Fut8*$^{-/-}$ primary fibroblasts, respectively.

^{125}I-TGF-β1-Binding Assays. The cells (1.5×10^5 per well) were cultured on 24-well plates, washed twice with 500 μl of PBS containing 0.1% BSA, and incubated with 200 μl of PBS containing different amounts of ^{125}I-TGF-β1 in a concentration range of 0.1–1.0 ng and 10 ng of unlabeled TGF-β1. Nonspecific binding was determined by adding 100 ng of unlabeled TGF-β1. After incubation for 2 h at 4°C with shaking, the cells were washed and solubilized in 500 μl of 1 M NaOH. The radioactivity of the cell lysates was counted with a γ-counter.

Receptor Cross-Linking. The cells (5×10^5) were seeded onto a 60-mm culture dish and incubated for 48 h. After being washed with cool PBS containing 0.1% BSA, the cells were incubated for 2 h at 4°C with 250 pM ^{125}I-TGF-β1 and then incubated with 1 mM cross-linking reagent BS^3 for 30 min at room temperature. After washing, the cells were lysed, the protein concentrations of cell lysates were determined, and the same amounts of protein were loaded onto 10% SDS-polyacrylamide gel for analysis. The gels were exposed and quantified with the BAS-2500 bio-imaging analyzer (Fuji).

Immunohistochemical Analysis. To detect the P-Smad2 (Ser-465/467), matrix metalloproteinase (MMP)-12, or SP-C, whole lung tissues from animals after age indicated were fixed in 0.1 M PBS containing 4% paraformaldehyde and embedded in paraffin. For immunohistochemical analysis, the dewaxed sections were pretreated with avidin-biotin blocking and hydroxygen blocking for 10 min at 37°C, and then incubated with rabbit anti-P-Smad2 antibody (Cell Signaling Technology, Beverly, MA), anti-MMP-12 antibody, or anti-SP-C antibody (Santa Cruz Biotechnology) for 16 h at 4°C. Localization of the first antibody was visualized by an avidin-biotin coupling (ABC) immunoperoxidase technique, using a commercial kit (Vector Laboratories) according to the manufacturer's instructions.

Therapeutic Administration of Exogenous TGF-β1 to *Fut8*$^{-/-}$ Mice. We performed i.p. injection of recombinant TGF-β1 in a dose of 5[illegible] or 100 ng/g of mouse body weight to postnatal 18-day *Fut8*$^{-/-}$ mice. After 20 times of injection every 2 days, lung sections were subjected to hematoxylin/eosin staining or immunohistochemical study.

Results and Discussion

***Fut8* Gene Is a Unique Fucosyltransferase Responsible for the Core Fucosylation of *N*-Glycans.** A targeted disruption of *Fut8* was generated through homologous recombination in embryonic stem cells. The targeting vector was constructed by replacing exon 2 of *Fut8*, which contains the translation initiation site, with an IRES-LacZ-Neo-pA cassette (Fig. 4*A*). Genotypes of pups from intercrosses between heterozygous mice were determined by Southern blotting (Fig. 4*B*). The phenotype described here was identical in two lines. Northern blot analysis of lung and brain RNA revealed that expression of full-length *Fut8* mRNA was abolished in homozygous mutant mice, whereas *Fut8* transcripts were detected as a single 3.5-kb band in wild-type mice (Fig. 4*C*). Consistent with this finding, Fut8 activity could not be detected in *Fut8*$^{-/-}$ tissues including brain or lung, even with six times longer incubation than that used for *Fut8*$^{+/+}$ specimens (Fig. 4*D* and data not shown). Furthermore, the analysis of *N*-glycan structures showed that the elution profile of *Fut8*$^{-/-}$ lung lacked the peaks of oligosaccharides with core fucose eluting at 30–35 min, as described in refs. 19 and 20 (Fig. 4*E*). These oligosaccharides were also confirmed by mass spectrometric analysis (Fig. 5, which is published as supporting information on the PNAS web site). This finding agrees with previous reports indicating that there are no additional genes homologous to *Fut8* in mammals and lower organisms (21, 22). Thus, the *Fut8* gene is the only one responsible for the core fucosylation of *N*-glycans in mouse tissues.

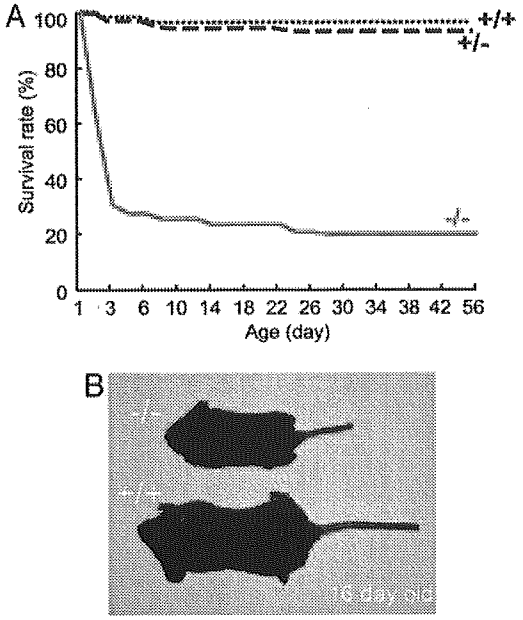

Fig. 1. Semilethality and growth retardation in *Fut8*$^{-/-}$ mice. (*A*) Survival ratio of *Fut8*$^{-/-}$ (−/−, solid line), *Fut8*$^{+/-}$ (+/−, broken line), and *Fut8*$^{+/+}$ (+/+, dotted line) mice after birth. (*B*) A 16-day-old *Fut8*$^{-/-}$ pup (−/−) with a *Fut8*$^{+/+}$ littermate (+/+).

Core Fucosylation Is Essential for Mice Survival and Growth. *Fut8*$^{-/-}$ mice were born apparently healthy with almost the expected Mendelian inheritance: Of 277 pups, there were 59 (21.3%) *Fut8*$^{-/-}$, 147 (53.1%) *Fut8*$^{+/-}$, and 71 (25.6%) *Fut8*$^{+/+}$ mice. At embryonic day 19, frequencies of *Fut8*$^{-/-}$, *Fut8*$^{+/-}$, and *Fut8*$^{+/+}$ mice were 26, 52, and 22 of 100 embryos, and there were no apparent anomalies in *Fut8*$^{-/-}$ mice. In contrast to *Fut8*$^{-/-}$ mice, embryonic lethality was observed in mutant mice deficient in the FX gene, which encodes an enzyme in the *de novo* pathway for GDP-fucose synthesis and is responsible for all cellular fucosylation, e.g., α1,2; α1,3; α1,6; etc. (23). The appearance of *Fut8*$^{-/-}$ mice could not be distinguished from *Fut8*$^{+/-}$ and *Fut8*$^{+/+}$ mice within 3 days of age, but ≈70% of them died during this period (Fig. 1*A*). Most of the survivors manifested severe growth retardation (Fig. 1*B*). This pattern observed in the *Fut8*$^{-/-}$ mice is quite different from other N-linked medial- and trans-Golgi glycosyltransferases, such as GnT-III-, GnT-V-, or ST6Gal1-null mice (14), suggesting that core fucose has a unique role in the regulation of proliferation and differentiation after birth.

Progressive Emphysema-Like Changes in *Fut8*$^{-/-}$ Lungs. Histological analyses by hematoxylin/eosin staining of 3-, 7-, 10-, and 18-day-old and 8-week-old *Fut8*$^{-/-}$ mice showed a symmetrical reduction in the size of most organs, which otherwise appeared devoid of pathological signs. The lungs of *Fut8*$^{-/-}$ mice, however, apparently displayed generalized air-space enlargement and dilated alveolar ducts, compared with those of *Fut8*$^{+/+}$ and *Fut8*$^{+/-}$ mice (Fig. 2*A*). The mean linear intercept was calculated at the ages indicated. From postnatal day 7, diameters of the pulmonary alveoli of *Fut8*$^{-/-}$ mice were increased significantly, compared with those in *Fut8*$^{+/+}$ mice (Fig. 2*B*). To evaluate the functional relevance of this morphological abnormality, lung compliance was evaluated by a static air deflation curve (Fig. 2*C*). The *Fut8*$^{-/-}$ lungs had larger total lung capacities and increased lung compliance compared with *Fut8*$^{+/-}$ and *Fut8*$^{+/+}$ lungs. These results indicate that the altered architecture of the enlarged *Fut8*$^{-/-}$ mouse airspace contributes to the increased compliance. We also measured pressure–volume relationships in body-weight-matched young wild types (≈7 days old) to cancel the difference in total lung capacity. Again, static lung compliance in *Fut8*$^{-/-}$ mice was greater than that in wild-type mice (data not shown). When *Fut8*$^{-/-}$ mice breathed room air under resting conditions, respiratory minute volume and rate, as determined by body plethysmography, were higher than in wild-type mice. Ventilatory responses to systemic hypoxia (12% O_2) or hypercapnia (5% CO_2/21% O_2), or increases in the respiratory minute volume, were significantly attenuated in *Fut8*$^{-/-}$ mice, compared with *Fut8*$^{+/+}$ and *Fut8*$^{+/-}$ mice (Fig. 2*D*). These findings, although not specific markers of emphysema, suggest that *Fut8* is involved in the physiological control of ventilation. However, we do not believe that the main reason that *Fut8*$^{-/-}$ mice die is lung disorder. Interestingly, besides TGF-β1 receptor as described below, we also found that loss of core fucosylation resulted in modest down-regulation of several other receptors-mediated signaling, such as EGF receptor and integrins (unpublished data), which are responsible for cell growth and differentiation. Therefore, we would like to take the hypothesis that the growth retardation and early death of *Fut8*$^{-/-}$ mice can be attributed to dysregulation of many receptors-mediated signaling.

Enhanced Expression Levels of MMPs in *Fut8*$^{-/-}$ Lungs and *Fut8*$^{-/-}$ Cells. Pulmonary emphysema is believed to result from decreased structural integrity of connective tissues due to a defect in their formation or to an abnormal proteolysis. Elastin and fibrillar collagen are major components of the extracellular matrix (ECM), which sustains the normal lung architecture. On the other hand, MMPs are a group of zinc- and calcium-dependent proteinases that have an important role in the normal turnover of ECM components. Abnormal production of MMPs is implicated in the induction of emphysema. Thus, transgenic mice expressing human MMP-1 develop emphysema through destruction of collagen fibrils (24). Furthermore, MMP-2, MMP-9, and MMP-12 lead to emphysema by degradation of elastin fibers (25, 26). Therefore, expression levels of collagens, elastin, and a number of MMPs of putative relevance in lung pathology, including McolB (a mouse orthologue of human MMP-1) (27) and MMP-2, -8, -9, -12, -13, and -14, were examined in the lungs of Fut8-mutant mice. RT-PCR analysis showed that there were no significant changes in the expression levels of collagens, MMP-2, -8, and -14 in lung tissues from *Fut8*$^{-/-}$, *Fut8*$^{+/-}$, and *Fut8*$^{+/+}$ mice (Fig. 3*A*). However, expression levels of McolB, MMP-12, and MMP-13 were greatly enhanced (Fig. 3*A*); in addition, a slight increase in MMP-9 levels was detected in lungs from *Fut8*$^{-/-}$ by using real-time RT-PCR (Fig. 6*A* and Table 2, which are published as supporting information on the PNAS web site). Conversely, elastin expression was down-regulated in lungs from Fut8-deficient mice. On the other hand, fragmentation and a significantly reduced number of elastic fibers were observed by elastin staining in *Fut8*$^{-/-}$ mice (Fig. 6*B*), supporting the view that the degrading phenotype, i.e., emphysematous changes, occurs in *Fut8*$^{-/-}$ lung. Actually, emphysema-like changes were coincident with increased expression levels of MMP-12 from postnatal day 7 of *Fut8*$^{-/-}$ mice (Fig. 6*C*). Furthermore, only in the bronchoalveolar lavage fluid of *Fut8*$^{-/-}$ mice did macrophages look vacuolated, which, along with MMP-12 expression, indicates activation (Fig. 6*I*). In addition, an enhanced expression of CD68, a marker of macrophage, was clearly observed in *Fut8*$^{-/-}$ lung (data not shown). Recently, Morris *et al.* (28) reported that the loss of the epithelial integrin $\alpha V\beta 6$, which causes a local deficiency in active TGF-β1, results in the increased expression of MMP-12 and leads to a slowly progressive, age-related emphysema. Likewise, McolB is a murine orthologue of human MMP-1, an enzyme that has been associated repeatedly with lung pathology, including emphysema (24), whereas MMP-13 or collagenase-3 is a very potent enzyme with wide substrate specificity, which is also associated with pulmonary diseases. It will also be interesting to examine whether core

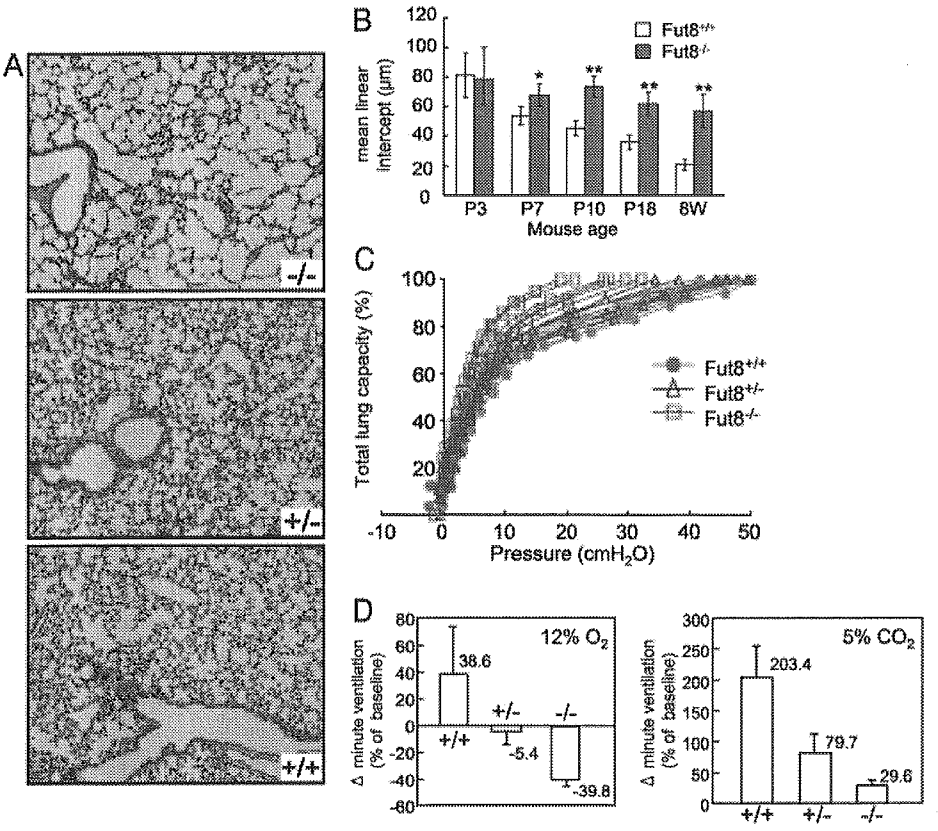

Fig. 2. Emphysematous change and impaired ventilatory response in *Fut8*$^{-/-}$ lung. (*A*) Representative histological sections (hematoxylin/eosin staining) of the lung of 18-day-old *Fut8*$^{+/+}$ (+/+), *Fut8*$^{+/-}$ (+/−), and *Fut8*$^{-/-}$ (−/−) pups show enlarged alveoli indicative of emphysema in *Fut8*$^{-/-}$ mice. (*B*) Lung morphometry at different stages. The mean linear intercepts of pulmonary alveoli were calculated at postnatal 3-, 7-, 10-, 18-day-old and 8-week-old mice. The diameters of the pulmonary alveoli were shown as the mean ± SD from three independent experiments. Statistical analysis was performed by using Student's *t* test. *, $P < 0.01$; **, $P < 0.001$ (versus the matched age of *Fut8*$^{+/+}$ mice). P, postnatal. (*C*) Lung compliance test. Static pressure–volume curves were plotted by using 19- to 20-day-old *Fut8*$^{-/-}$ (brown), *Fut8*$^{+/+}$ (pink), and *Fut8*$^{+/-}$ (blue) pups. (*D*) Comparison of changes in respiratory minute volume in response to hypoxic or hypercapnic air in conscious 19- to 20-day-old littermate *Fut8*$^{+/+}$ (+/+), *Fut8*$^{+/-}$ (+/−), and *Fut8*$^{-/-}$ (−/−) mice.

fucosylation affects MMP proteolytic function, because some MMPs such as MMP-9 contain *N*-glycans with core fucose. Taken together, these results suggest that overexpression of a set of MMPs might be causally linked to the development of emphysema in *Fut8*$^{-/-}$ mice.

To gain insight into the mechanism of induction of these MMPs in *Fut8*$^{-/-}$ mice, we established embryonic fibroblasts from *Fut8*$^{+/+}$ and *Fut8*$^{-/-}$ mice. Consistent with the data from the lungs shown in Fig. 3*A*, under resting conditions, McolB mRNA transcripts (Fig. 3*B*) and MMP-12 (Fig. 3*C*) and MMP-13 (data not shown) proteins secreted into the media were barely detected in wild-type embryonic fibroblasts, whereas they were clearly detected in *Fut8*$^{-/-}$ cells. To examine whether these changes in MMP expression levels were also manifested in the respective MMP proteolytic activities, gelatin and casein zymographies were performed by using the conditioned media from these embryonic cells. A differential band of ≈45 kDa, likely corresponding to the gelatinolytic activity of MMP-12, was observed in the gelatin zymogram of *Fut8*$^{-/-}$ cells. Likewise, a band of ≈55 kDa was detected in the casein zymogram of *Fut8* $^{-/-}$ cells (Fig. 6 *D* and *E*). In fact, the increased expression levels of both MMP-12 and MMP-13 secreted into media in the *Fut8*$^{-/-}$ cells were also confirmed by a Western blot (Fig. 6*F*). Consistent with these results, the enhancement of MMP-12 expression was also observed in lung tissues of *Fut8* $^{-/-}$ mice (Fig. 6*G*). These results demonstrate that the increased RNA and protein expression levels of some MMPs are accompanied by an increase in the proteolytic potential of cells from *Fut8*-deficient mice.

Lack of Core Fucose in TGF-β Receptor Leads to Inhibiting Its Function. Recently, it became clear that modification by N-glycosylation can affect the biological functions of many glycoprotein receptors. As described above, we found that loss of core fucosylation resulted in down-regulation of several receptor-mediated signaling pathways, such as TGF-β1 receptor, EGF receptor, and integrins, which are responsible for cell growth and differentiation, and also emphysema. The TGF-β1 receptor-mediated signaling pathway is a key pathway for regulating expression of ECM proteins, including suppression of MMPs to produce a "synthetic" phenotype (29). When the embryonic fibroblasts were treated with IL-1β, which enhances MMP expression, McolB mRNA levels were elevated markedly in both *Fut8*$^{+/+}$ cells and *Fut8*$^{-/-}$ cells (Fig. 3*B*). The enhancement of McolB expression stimulated by IL-1β was blocked by TGF-β1 treatment in *Fut8*$^{+/+}$ cells but not in *Fut8*$^{-/-}$ cells (Fig. 3*B*), indicating that the deletion of *Fut8* does not alter IL-1β-receptor-mediated function but diminishes TGF-β1-mediated signaling. The decreased response of TGF-β1 stimulation was also observed in protein expression levels of MMP-12 secreted into the media (Fig. 3*C*). To examine how core fucose affects TGF-β1-mediated signaling, we measured the binding activity of TGF-β1 for its surface receptor. The binding ability of ^{125}I-TGF-β1 was reduced significantly in *Fut8*$^{-/-}$ cells compared with *Fut8*$^{+/+}$ cells, which could be rescued by reintroducing *Fut8* to *Fut8*$^{-/-}$ cells (Fig. 3*D*). Consistent with this, the amount of TGF-β1 bound and cross-linked to type I, II, and III receptors was suppressed dramatically in *Fut8*$^{-/-}$ cells; these features were recovered by reintroducing *Fut8* to *Fut8*$^{-/-}$ cells (Fig. 3*E*). Actually, the levels of core fucosylation

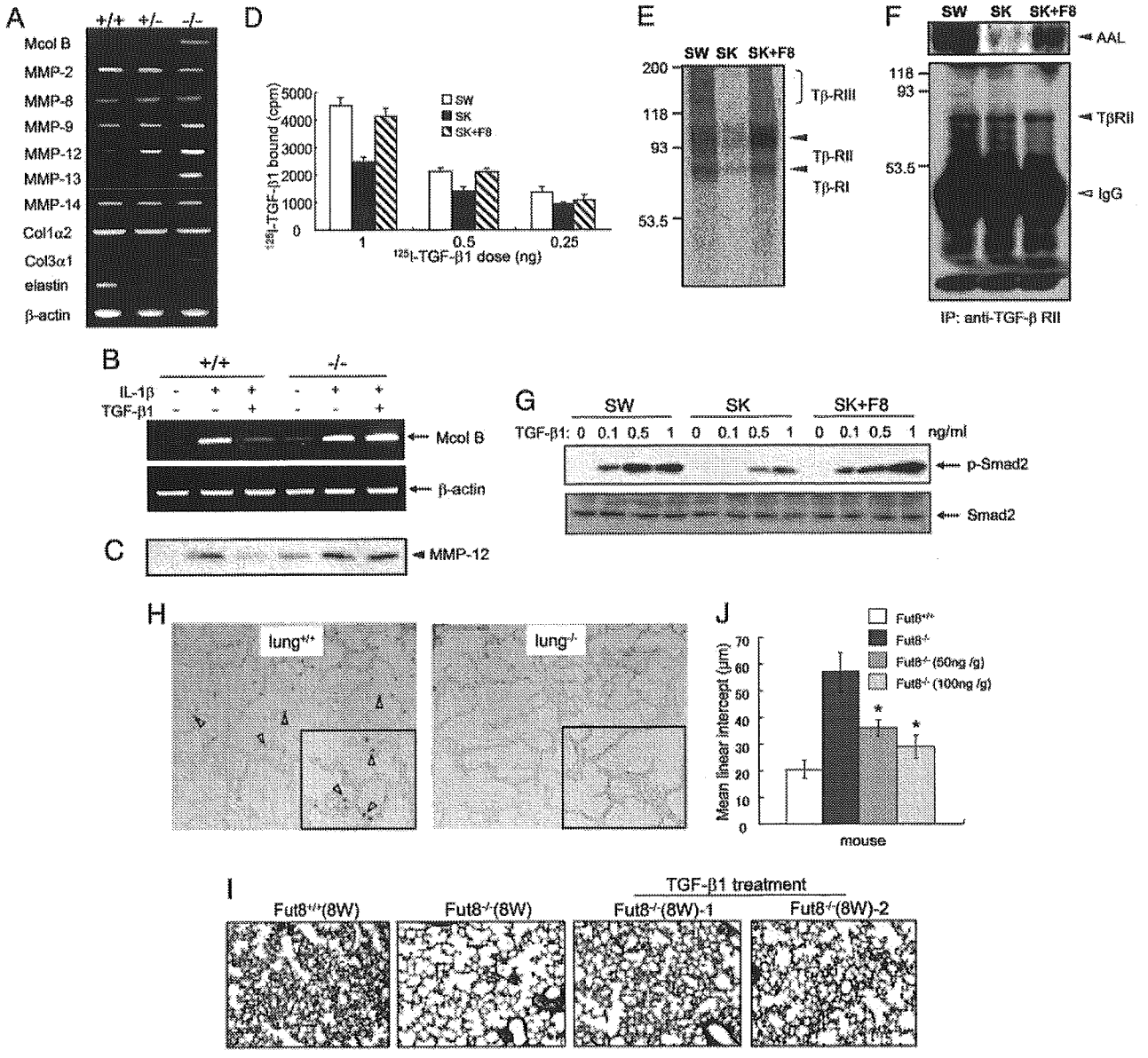

Fig. 3. Enhancement of some MMPs expression through down-regulation of TGF-β-receptor-mediated signaling in *Fut8*$^{-/-}$ lung and embryonic fibroblasts. (*A*) RT-PCR analysis of emphysema-relating genes (see Table 1, which is published as supporting information on the PNAS web site). Total RNAs from 18-day-old *Fut8*$^{+/+}$ (+/+), *Fut8*$^{+/-}$ (+/−), and *Fut8*$^{-/-}$ (−/−) lungs were used as template. β-Actin RNA is shown as a loading control. (*B*) Effects of IL-1β and TGF-β1 on McolB expression. These fibroblasts were preincubated with or without TGF-β1 (1 ng/ml) for 3 h and then further incubated with or without IL-1β (2 ng/ml) for 24 h. Total RNA was isolated and used as template. (*C*) Effects of IL-1β and TGF-β on protein expression of MMP-12 secreted into culture media. These fibroblasts were incubated with or without IL-1β and TGF-β1 in the absence of FCS. After incubation for 24 h, the conditioned media were concentrated and subjected to electrophoresis for Western blot. (*D*) Binding of ^{125}I-TGF-β1 to its receptors on the cell surface. These cells from *Fut8*$^{+/+}$ (+/+) and *Fut8*$^{-/-}$ (−/−) primary fibroblasts immortalized with SV40 large T, SW, and SK, respectively, or SK restored with *Fut8* (SK+F8), were incubated with different amounts of radiolabeled TGF-β1 as indicated and 10 ng of cold TGF-β1 for 2 h on ice. Cell lysate radioactivity was measured. (*E*) ^{125}I-TGF-β1 was bound and cross-linked to its receptors on cell surface. The cultured cells were incubated with 250 pM ^{125}I-TGF-β1 for 2 h at 4°C, and then cross-linked with reagent BS^3. (*F*) Analysis of fucosylation levels on TGF-β receptor II. TGF-β1 receptor II was immunoprecipitated from whole-cell lysates and then subjected to electrophoresis on 8% SDS/PAGE. After electroblotting, blots were probed by ALL lectin (*Upper*) and anti-TGF-β receptor II (*Lower*). (*G*) Effects of phosphorylated Smad2 levels on TGF-β1 stimulation. Serum-starved cells were treated with or without TGF-β1 at the indicated concentrations for 5 min and solubilized in lysis buffer as described in *Materials and Methods*. The cell lysates were detected by immunoblotting of anti-phospho-Smad2 antibody (*Upper*) and anti-Smad2 antibody (*Lower*). (*H*) The lung sections of 4-day-old mice were pretreated with hydroxygen blocking for 10 min at 37°C and then incubated with rabbit anti-human P-Smad2 antibody for 16 h at 4°C. The arrowheads indicate positive staining in *Fut8*$^{+/+}$ lung. (*I*) Therapeutic administration of recombinant TGF-β1 rescues emphysema-like changes in *Fut8*$^{-/-}$ mice. The surviving postnatal 18-day-old *Fut8*$^{-/-}$ mice were treated with or without recombinant TGF-β1 (50 or 100 ng/g of mouse body weight) for 20 times of injection every 2 days, and then the lung sections were subjected to hematoxylin/eosin staining. (*J*) Quantitative analyses of the pulmonary alveolar sizes were performed by mean linear intercept as described above. The diameters of the pulmonary alveoli were shown as the mean ± SD from three independent experiments. Statistical analysis was performed by using Student's *t* test. *, $P < 0.01$ (*Fut8*$^{-/-}$ mice treated with TGF-β versus the matched age of mice without treatment).

detected by AAL lectin in the TGF-β type II receptor, which is the primary binding subunit for TGF-β1 (30–32), were abolished in *Fut8*$^{-/-}$ cells, whereas they were recovered by restoring *Fut8* (Fig. 3*F*). The TGF-β1 signaling via receptors to intracellular mediators of the Smad family was suppressed significantly in *Fut8*$^{-/-}$ cells (Fig. 3*G*). Smad2 is a direct substrate for the activated TGF-β type